Large Contributions from Biogenic Monoterpenes and Sesquiterpenes to Organic Aerosol in the Southeastern United States

Lu Xu[1,a], Havala O.T. Pye[2], Jia He[3], Yunle Chen[4], Benjamin N. Murphy[2], Nga Lee Ng[1,3*]

[1]School of Chemical and Biomolecular Engineering, Georgia Institute of Technology, Atlanta, GA 30332, USA

[2]National Exposure Research Laboratory, US Environmental Protection Agency, Research Triangle Park, NC 27711, USA

[3]School of Earth and Atmospheric Sciences, Georgia Institute of Technology, Atlanta, GA 30332, USA

[4]School of Materials Science and Engineering, Georgia Institute of Technology, Atlanta, GA 30332, USA

[*]To whom correspondence should be addressed. E-mail: ng@chbe.gatech.edu

[a]Present address: Division of Geological and Planetary Sciences, California Institute of Technology, Pasadena, CA 91125, USA

Abstract

Atmospheric organic aerosol (OA) has important impacts on climate and human health but its sources remain poorly understood. Biogenic monoterpenes and sesquiterpenes are critical precursors of OA. The OA generation from these precursors predicted by models has considerable uncertainty owing to a lack of appropriate observations as constraints. In this study, we propose that the less-oxidized oxygenated organic aerosol (LO-OOA) factor resolved from positive matrix factorization (PMF) analysis on aerosol mass spectrometry (AMS) data can be used as a surrogate for fresh SOA from monoterpenes and sesquiterpenes in the southeastern U.S. We support this hypothesis based on a weight of evidence, including lab-in-the-field perturbation experiments, extensive ambient ground-level measurements, and state-of-the-art modeling. We performed lab-in-the-field experiments, in which the ambient air is perturbed by the injection of selected monoterpenes and sesquiterpenes and subsequent SOA formation. PMF analysis on the perturbation experiments provides an objective link between LO-OOA and fresh SOA from monoterpenes and sesquiterpenes as well as insights into the sources of other OA factors. Further, we use an upgraded atmospheric model and show that modeled SOA concentrations from monoterpenes and sesquiterpenes could reproduce both the magnitude and diurnal variation of LO-OOA at multiple sites in the southeastern U.S., building confidence in our hypothesis. We predict the annual average concentration of SOA from monoterpenes and sesquiterpenes in the southeastern U.S. is ~2.1 μg m^{-3}. This amount is substantially higher than represented in current regional models and accounts for 21% of World Health Organization $PM_{2.5}$ standard, indicating a significant contributor of environmental risk to the 77 million habitants in the southeastern U.S.

1 Introduction

Organic aerosol (OA) constitutes a substantial fraction of ambient fine particulate matter (PM) and has large impacts on air quality, climate change, and human health (Carslaw et al., 2013; Lelieveld et al., 2015). OA can be directly emitted from sources (primary OA, POA) or formed by the oxidation of volatile organic compounds (VOCs) (secondary OA, SOA). Global measurements revealed the dominance of SOA over POA in various atmospheric environments (Jimenez et al., 2009; Ng et al., 2010). The VOCs can be emitted from natural sources (i.e., biogenic) or human activities (i.e., anthropogenic). However, the relative contribution of biogenic and anthropogenic sources to SOA formation in the atmosphere is poorly constrained. This knowledge is critical for formulating effective pollution control strategies that aim at reducing ambient PM concentrations and accurately assessing the climate effects of OA (Hallquist et al., 2009). Biogenic VOCs such as monoterpenes (MT, $C_{10}H_{16}$) and sesquiterpenes (SQT, $C_{15}H_{24}$) are recognized as critical precursors of SOA (Tsigaridis et al., 2014; Hodzic et al., 2016; Pye et al., 2010). The predicted global SOA production from MT and SQT varies from 14 to 246 Tg yr^{-1} (Spracklen et al., 2011; Pye et al., 2010). This large variation in model estimates arises from a number of factors (including uncertainty in SOA yield) and introduces significant uncertainties in estimating OA concentrations and its subsequent influences on climate and human exposure.

The large model uncertainties call for ambient observations to constrain model results. Isolating and measuring SOA production from specific sources are challenging because SOA is a complex mixture consisting of thousands of compounds and SOA evolves dynamically in the atmosphere. A widely used method to apportion OA into different characteristic sources is positive matrix factorization (PMF) analysis on the organic mass spectra measured by aerosol mass spectrometer (AMS) (Ulbrich et al., 2009; Jimenez et al., 2009; Ng et al., 2010). PMF-AMS analysis groups OA constituents with similar mass spectra and temporal variations into characteristic OA subtypes (i.e., factors). This analysis has revealed that concentration of oxygenated OA (OOA), which is a surrogate of SOA, is much greater than that of hydrocarbon-like OA (HOA), which is a surrogate of POA (Zhang et al., 2007). In many circumstances especially in warmer months, more than one SOA factor is resolved from PMF analysis, often including less-oxidized oxygenated OA (LO-OOA, also denoted as semi-volatile oxygenated organic aerosol in older studies) and more-oxidized oxygenated OA (MO-OOA, also denoted as low-volatility oxygenated organic aerosol in older studies). LO-OOA and MO-OOA are

differentiated by their degree of carbon oxidation. These two factors together account for more than half of total submicron OA (Crippa et al., 2014; Xu et al., 2015a; Jimenez et al., 2009). Despite of their large abundance, the sources of LO-OOA and MO-OOA are unclear and likely vary with location and season. Early studies, primarily based on comparison of the mass spectra of OA factors with those of laboratory-generated SOA, proposed that LO-OOA is freshly formed SOA from various sources and evolves into MO-OOA with photochemical aging in the atmosphere (Jimenez et al., 2009; Ng et al., 2010). Later, a number of possible sources have been proposed for MO-OOA, including SOA from long-range transport (Hayes et al., 2013; Robinson et al., 2011b), aged biomass burning OA (Bougiatioti et al., 2014; Grieshop et al., 2009), humic-like substances (El Haddad et al., 2013), highly oxygenated molecules (HOMs) formed in the oxidation of monoterpenes (Mutzel et al., 2015; Ehn et al., 2014), and aqueous phase processing (Xu et al., 2016c). Regarding the sources of LO-OOA, Zotter et al. (2014) applied radiocarbon analysis and showed that 68-75% of carbon in LO-OOA in California stems from fossil sources. In the southeastern U.S., Xu et al. (2015a) suggested that the oxidation of biogenic β-pinene by nitrate radicals (NO_3) contributes to LO-OOA, though this reaction alone cannot replicate the magnitude of LO-OOA (Pye et al., 2015). These studies significantly advanced our knowledge of the sources and evolution of ambient OA; however, uncertainties associated with the sources of these OA factors still exist. As a result, atmospheric models typically use the lumped LO-OOA and MO-OOA concentration to constrain simulated total SOA concentration (Spracklen et al., 2011; Tsigaridis et al., 2014), which hinders our ability to diagnose the cause of discrepancies between modeled and observed aerosol concentrations (Spracklen et al., 2011). Many sources of LO-OOA and MO-OOA are proposed based on comparing the mass spectra between OA factors and laboratory-generated SOA (Jimenez et al., 2009; Palm et al., 2018; Kiendler-Scharr et al., 2009). However, the similarity between two mass spectra is a subjective determination. Further, the subjectively-defined similarity cannot tell what is the fraction of SOA from a certain source contributes to one OA factor. Overall, considering the large abundance of OOA subtypes and their use as surrogates for ambient SOA, understanding the sources of compounds composing these two OA subtypes is critical to constrain atmospheric models and the SOA budget.

In this study, we integrate lab-in-the-field experiments, extensive ambient ground measurements, and state-of-the-art modeling to improve the understanding of the sources of OA factors and better constrain the OA budget from MT and SQT. Based on lab-in-the-field

experiments, we provide objective evidence that newly formed SOA from α-pinene (an important monoterpene) and β-caryophyllene (an important sesquiterpene) is dominantly apportioned to LO-OOA in the southeastern U.S. In addition, we model the SOA concentration from the oxidation of MT and SQT (denoted as SOA_{MT+SQT}) and show that SOA_{MT+SQT} reasonably reproduces the magnitude and diurnal variability of LO-OOA measured at multiple sites in the southeastern U.S. Together with other evidence in the literature, we propose that LO-OOA can be used as a measure of SOA_{MT+SQT} in the southeastern U.S. Finally, we discuss how the lab-in-the-field approach allows for the study of SOA formation under realistic atmospheric conditions, which bridges laboratory studies and field measurements and provides a direct way to evaluate the atmospheric relevancy of laboratory studies.

2 Method

2.1 Lab-in-the-field perturbation experiments

The perturbation experiments were performed in July-August 2016 on the rooftop of the Environmental Science and Technology building on the Georgia Institute of Technology campus. This measurement site is an urban site in Atlanta, Georgia. Multiple ambient field studies have been performed at this site previously (Xu et al., 2015b; Hennigan et al., 2009; Verma et al., 2014). A $2m^3$ Teflon chamber (cubic shape) (Fig. 1) was placed outdoor on the rooftop of the building. The eight corners of the chamber were open (~2"×2") to the atmosphere to allow for continuous exchange of air with the atmosphere. The perturbation procedure is briefly described below and illustrated in Fig. A1. Firstly, we continuously flushed the chamber with ambient air using two fans, which were placed at two corners of the chamber. During this flushing period, all instruments sampled ambient air and were not connected to the chamber. The flushing period lasted at least 3 hours to ensure that the air composition in the chamber is the same as ambient composition. Secondly, we stopped both fans and connected all instruments to chamber. Because of the continued sampling by the instruments (~20 liter per minute) and the open corners of the chamber, ambient air continuously entered the chamber, even though the two fans were turned off. Thirdly, after sampling the chamber for about 30min, we injected a known amount of VOC (liquid) into the chamber with a needle, where the liquid vaporized upon injection. We continuously monitored the chamber composition for ~40 min after VOC injection. Lastly, we disconnected all instruments

from the chamber, sampled ambient air, and turned on two fans to flush the chamber to prepare for the next perturbation experiment.

Each perturbation experiment can be divided into the following four periods: Amb_Bf (30min ambient measurement period before sampling chamber), Chamber_Bf (from sampling chamber to VOC injection, a period ~30min), Chamber_Af (from VOC injection to stop sampling chamber, a period ~40min), and Amb_Af (30min ambient measurement period after sampling chamber). We calculate the changes in the mass concentration of OA factors after perturbation based on the difference between Chamber_Bf and Chamber_Af, after taking ambient variation into account. The detailed procedure is presented in Appendix A. We develop a comprehensive set of criteria to determine if the changes are statistically significant and if the changes are simply due to ambient variations. The details of these criteria are also discussed in Appendix A.

We perturbed the chamber content by injecting one of the following VOCs: isoprene, α-pinene, β-caryophyllene, *m*-xylene, or naphthalene, which are major biogenic or anthropogenic emissions. We focused on α-pinene and β-caryophyllene, because they are widely studied in the literature (Eddingsaas et al., 2012a; Kurtén et al., 2015; Tasoglou and Pandis, 2015; Ehn et al., 2014; Pathak et al., 2007) and they have large abundances in their classes. For example, α-pinene accounts for about half of monoterpenes emissions (Guenther et al., 2012) and β-caryophyllene is one of the most abundant sesquiterpenes (Helmig et al., 2007). The injected VOC amounts were carefully selected. If the injection amount is too large, it is not atmospherically relevant, produces too much SOA, and will bias subsequent analysis. If the injection amount is too small, the produced SOA would fall below the detection limit of the experimental approach. The VOC oxidation occurred in ambient air (inside the chamber) and lasted ~40 min. The OA concentration in the chamber after perturbation ranges from 4 to 16 $\mu g\ m^{-3}$, which is within the range of typical ambient OA concentrations.

We note that several previous studies have used ambient air (Palm et al., 2017; Leungsakul et al., 2005; Peng et al., 2016), but experimental approaches and purposes of previous studies are different from this study. For example, In Leungsakul et al. (2005), the rural ambient air was used to flush and clean the $270 m^3$ outdoor chamber reactor. After the flushing, both VOCs and oxidants were injected to produce SOA, the concentration of which were orders of magnitude higher than atmospheric levels. In this study, we use ambient air with pre-existing OA in order to examine

which factor(s) the fresh α-pinene and β-caryophyllene SOA are apportioned into by PMF analysis. We aim to produce SOA only from injected α-pinene or β-caryophyllene, so that an important distinction between our study and pervious work is that we perturbed the ambient air by only VOCs, not extra oxidant.

2.2 Analytical instruments

A suite of analytical instruments was deployed to characterize both the gas-phase and particle-phase compositions. The particle-phase composition was monitored by a scanning mobility particle sizer (SMPS, TSI) and a high resolution time-of-flight aerosol mass spectrometer (HR-ToF-AMS, Aerodyne), which shared the same stainless steel sampling line. A diaphragm pump (flow rate ~8 liter per minute) was connected to this sampling line, which increased the sampling flow rate and reduced particle loss in the sampling line by reducing the residence time in the tubing. The HR-ToF-AMS measures the chemical composition and size distribution of submicron non-refractory species (NR-PM_1) with high temporal resolution. The instrument details about HR-ToF-AMS have been extensively discussed in the literature (Canagaratna et al., 2007; DeCarlo et al., 2006) and the operation of HR-ToF-AMS in this study is described in the section S2 of Supplement.

The gas-phase composition and oxidation products was monitored by an O_3 analyzer (Teledyne T400, lower detectable limit 0.6ppb), an ultrasensitive chemiluminescence NO_x monitor (Teledyne 200EU, lower detectable limit 50ppt), and a high-resolution time-of-flight chemical ionization mass spectrometer (HR-ToF-CIMS). The HR-ToF-CIMS with I^- as regent ion can measure a suite of oxygenated volatile organic compounds (oVOCs) at high frequency (1Hz). Detailed working principles and sampling protocol can be found in Lee et al. (2014). The concentrations of VOCs were not measured in this study. All gas-phase measurement instruments shared the same Teflon sampling line. Similar to the particle sampling line, a diaphragm pump (flow rate ~8 liter per minute) was connected to the gas sampling line to reduce the residence time in the tubing.

2.3 Positive Matrix Factorization (PMF) analysis

PMF analysis has been widely used for aerosol source apportionment in the atmospheric chemistry community (Jimenez et al., 2009; Crippa et al., 2014; Xu et al., 2015a; Ng et al., 2010; Ulbrich et al., 2009; Beddows et al., 2015; Visser et al., 2015). PMF solves bilinear unmixing factor model by minimizing the summed least squares errors of the fit weighted with the error estimates of each

measurement (Paatero and Tapper, 1994; Ulbrich et al., 2009). We utilized the PMF2 solver, which does not require a priori information and reduces subjectivity. In this study, we performed PMF analysis on the high-resolution mass spectra of organic aerosol (inorganic species are excluded) of combined ambient and perturbation data in the one-month measurements. Considering that (1) the perturbation data only account for ~10% of total data and (2) the OA concentration is similar between the perturbation experiments and typical ambient measurements, the perturbation experiments do not create a new factor that does not already exist in the ambient data. This is desirable because it allows PMF analysis to apportion the newly formed OA in the perturbation experiments into pre-existing OA factors in the atmosphere.

We resolved five OA factors, including hydrocarbon-like OA (HOA), cooking OA (COA), isoprene-derived OA (isoprene-OA), less-oxidized oxygenated OA (LO-OOA), and more-oxidized oxygenated OA (MO-OOA). The time series and mass spectra of OA factors are shown in Fig. 2. The same 5 factors have been identified at the same measurement site and extensively discussed in the literature (Xu et al., 2015a; Xu et al., 2015b; Xu et al., 2017). Below, we only provide a brief description on these OA factors and more details are discussed in section S3 of Supplement. The mass spectrum of HOA is dominated by hydrocarbon-like ions ($C_xH_y^+$ ions) and HOA is a surrogate of primary OA from vehicle emissions (Zhang et al., 2011). For COA, its concentration is higher at meal times and its mass spectrum is characterized by prominent signal at ions $C_3H_5^+$ (*m/z* 41) and $C_4H_7^+$ (*m/z* 55), which likely arise from fatty acids (Huang et al., 2010; Mohr et al., 2009; Allan et al., 2010). The mass spectrum of isoprene-OA is characterized by prominent signal at ions $C_4H_5^+$ (*m/z* 53) and $C_5H_6O^+$ (*m/z* 82) and it is related to the reactive uptake of isoprene oxidation products, isoprene epoxydiols (IEPOX) (Budisulistiorini et al., 2013; Hu et al., 2015; Robinson et al., 2011a; Xu et al., 2015a). LO-OOA and MO-OOA are named based on their differing carbon oxidation state, that is, from -0.70 to -0.34 for LO-OOA and from -0.18 to 0.71 for MO-OOA in the southeastern U.S. (Xu et al., 2015b). We performed 100 bootstrapping runs to quantify the uncertainty of PMF results. As shown in Fig. S1, the statistical uncertainties in the time series and mass spectra of 5 factors are small and the PMF results reported in this study are robust.

2.4 Details of multiple ambient sampling sites

Measurements at multiple sites in the southeastern U.S. were performed as part of Southeastern Center for Air Pollution and Epidemiology study (SCAPE) and Southern Oxidant and Aerosol Study (SOAS) in 2012 and 2013. Detailed descriptions about these field studies have been discussed in the literature (Xu et al., 2015a; Xu et al., 2015b) and section S4 of Supplement. The sampling periods are shown in Table S1 and the sampling sites are briefly discussed below.

• Georgia Tech site (GT): This site is located on the rooftop of the Environmental Science and Technology building on the Georgia Institute of Technology (GT) campus, which is about 30-40m above the ground and 840m away from interstate I75/85. This is an urban site in Atlanta. This is also where the perturbation experiments in this study were conducted.

• Jefferson Street site (JST): This is a central SEARCH (SouthEastern Aerosol Research and Characterization) site, which is in Atlanta's urban area with a mixed commercial and residential neighborhood. It is about 2 km west of the GT site. The JST and GT sites are in the same grid cell in CMAQ.

• Yorkville site (YRK): This is a central SEARCH site located in a rural area in Georgia. This site is surrounded by agricultural land and forests and is at about 80 km northwest of JST site.

• Centreville site (CTR): This is a central SEARCH site in rural Alabama. The sampling site is surrounded by forests and away from large urban areas (55km SE and 84 km SW of Tuscaloosa and Birmingham, AL, respectively). The is the main ground site for the SOAS campaign.

2.5 Laboratory chamber study on SOA formation from α-pinene

To compare with results from the lab-in-the-field perturbation experiments, we performed laboratory experiments to study the SOA formation from α-pinene photooxidation under different NO_x conditions in the Georgia Tech Environmental Chamber (GTEC) facility. The facility consists of two 12 m^3 indoor Teflon chambers, which are suspended inside a temperature-controlled enclosure and surrounded by black lights. The detailed description about chamber facility can be found in Boyd et al. (2015). The experimental procedures have been discussed in Tuet et al. (2017). In brief, the chambers were flushed with clean air prior to each experiment. Then, α-pinene and oxidant sources (i.e., H_2O_2, NO_2, or HONO) were injected into chamber. Once the concentrations of species stabilize, the black lights were turned on to initiate photooxidation. The experimental conditions are summarized in Table S2. Considering that the OA mass concentration affects the

partitioning of semi-volatile organic compounds (Odum et al., 1996) and hence affects the organic mass spectra measured by AMS, we calculated the average mass spectra in these laboratory studies by only using the data when the OA mass concentration is below 10 μg m^{-3}, which is similar to that in our ambient perturbation experiments.

2.6 Community Multiscale Air Quality (CMAQ) Model

We used the Community Multiscale Air Quality (CMAQ) atmospheric chemical transport model to simulate the pollutant concentrations across the southeastern U.S. CMAQ v5.2gamma was run over the continental U.S. for time periods between May 2012 to July 2013 with 12km × 12km horizontal resolution. We focus our analysis on the southeastern U.S., which comprises 11 states (Arkansas, Alabama, Florida, Georgia, Kentucky, Louisiana, Mississippi, North Carolina, South Carolina, Tennessee, and Virginia). The meteorological inputs were generated with version 3.8 of the Weather Research and Forecasting model (WRF), Advanced Research WRF (ARW) core. We also applied lightning assimilation to improve convective rainfall (Heath et al., 2016). Anthropogenic emissions were based on the EPA (Environmental Protection Agency) NEI (National Emission Inventory) 2011 v2. Biogenic emissions were predicted by the BEIS (Biogenic Emission Inventory System) v3.6.1. The gas-phase chemistry was based on CB6r3 (Carbon Bond v6.3).

We performed two simulations with different organic aerosol treatment. The "default simulation" generally follows the scheme of Carlton et al. (2010), with the addition of IEPOX SOA following Pye et al. (2013) and documented in Appel et al. (2017) (Fig. S2a). The traditional two-product absorptive partitioning scheme (Odum et al., 1996) is used in "default simulation" to describe SOA formation from monoterpenes using data from laboratory experiments by Griffin et al. (1999). In the "updated simulation", we incorporate two recent findings. Firstly, we implemented MT+NO_3 chemistry to explicitly account for the organic nitrate compounds that have recently been shown to be a ubiquitous and important component of OA (Pye et al., 2015; Kiendler-Scharr et al., 2016; Lee et al., 2016; Ng et al., 2017). We follow the scheme described in Pye et al. (2015) to represent the formation and partition of organic nitrates from monoterpenes via multiple reaction pathways (i.e., oxidation by NO_3 and oxidation by OH/O_3 followed by RO_2+NO). Secondly, we improved the parameterization of SOA formation from MT+O_3/OH based on a recent study by Saha and Grieshop (2016), who applied a dual-thermodenuder system

to study the α-pinene ozonolysis SOA. The authors extracted parameters (i.e., SOA yields and enthalpies of evaporation) by using an evaporation-kinetics model and volatility basis set (VBS). The SOA yields in Saha and Grieshop (2016) are consistent with recent findings on the formation of HOMs (Ehn et al., 2014; Zhang et al., 2015) and help to explain the observed slow evaporation of α-pinene SOA (Vaden et al., 2011). In the updated simulation, we use the VBS framework with parameters derived from Saha and Grieshop (2016). The new parameterization allows for enthalpies of vaporization that are more consistent with species of the specified volatility. The properties of the volatility bins in the VBS framework are listed in Table S3. A schematic of SOA treatment in "updated simulation" is shown in Fig. S2b. In the following discussions, we focus on the results from "updated simulation". The comparison between "default simulation" and "updated simulation" can be found in the section S5 of Supplement.

3 Results and Discussions

3.1 α-pinene perturbation experiments

A total of 19 α-pinene perturbation experiments were performed at different times of the day (i.e., from 9am to 9pm) to probe a wide range of reaction conditions. The injection time and concentrations of O_3 and NO_x during α-pinene perturbation experiments are summarized in Table S4. Based on the chamber volume and injected liquid α-pinene volume, initially ~14 ppb α-pinene is injected into chamber. Due to lack of VOC measurements, we build a box model to simulate the fate of α-pinene in the chamber (section S6 of Supplement). We estimate that only a small fraction (2-5ppb) of α-pinene is reacted in the chamber and most of α-pinene is carried out of the chamber due to dilution with ambient air.

Fig. 3 shows the time series of OA factors in a typical α-pinene perturbation experiment. An evident burst and increase of LO-OOA after α-pinene injection occurs. This provides direct evidence that freshly formed α-pinene SOA contributes to LO-OOA. About 15 min after α-pinene injection, LO-OOA concentration starts to decrease, as ambient air continuously flows into the chamber and dilutes the concentration of LO-OOA (section S6 of Supplement). As shown in Fig. S3, the major known gas-phase oxidation products of α-pinene measured by HR-ToF-CIMS (Eddingsaas et al., 2012b; Lee et al., 2016; Yu et al., 1999) show an immediate increase after α-pinene injection. This verifies the rapid oxidation of α-pinene in the chamber.

Fig. 4a shows the perturbation-induced changes in the concentrations of OA factors for all α-pinene experiments. Out of 19 experiments, the LO-OOA concentration is enhanced in 14 experiments. Also, among all OA factors, LO-OOA shows the largest enhancement. This directly supports that freshly formed α-pinene SOA contributes to LO-OOA. The enhancement in LO-OOA concentration differs between experiments, mainly because the perturbations were performed at different times of day (i.e., from 9am to 9pm) and with different reaction variables (i.e., temperature, relative humidity, oxidants concentrations, NO_x, etc). Despite the large difference in reaction conditions, we note that both LO-OOA enhancement amount and LO-OOA formation rate (i.e., slope of LO-OOA increase) correlate positively with ozone concentration (Fig. 5). This correlation suggests that the concentration of oxidants, both ozone and hydroxy radical (OH, which is not measured in this study but is known to positively correlate with ozone in the atmosphere), plays a more controlling role in the amount of OA formed in α-pinene experiment than other reaction variables do. This is likely because higher oxidant concentrations lead to more α-pinene consumption and hence more OA production with the same reaction time.

MO-OOA only increases in 1 out of 19 α-pinene experiments. The highly oxygenated molecules (HOMs), which are rapidly produced from the oxidation of α-pinene, are a hypothesized source of MO-OOA, because of the high O:C ratio of HOMs (Ehn et al., 2014; Mutzel et al., 2015). However, HOMs are first generation monoterpene products co-formed with semivolatile SOA species, and the lack of enhancement in MO-OOA suggests that the HOMs are unlikely contributors to MO-OOA. We cannot rule out the possibilities that HOMs are not formed under our experimental conditions, and future studies on the simultaneous verification of HOMs formation and apportion of HOMs by PMF analysis are warranted.

Isoprene-derived OA (isoprene-OA) increases in 7 out of 19 α-pinene experiments. This increase is surprising because the isoprene-OA factor (also referred to as "IEPOX-OA" in some studies) is typically interpreted as SOA from the reactive uptake of IEPOX, but our results suggest that the isoprene-OA factor could have interferences from α-pinene SOA. The isoprene-OA enhancement is due to interference from newly formed α-pinene SOA, rather than that the injected α-pinene affecting the oxidation of pre-existing isoprene or affecting the gas/particle partitioning of pre-existing semi-volatile species in the chamber, because of the following reasons. Firstly, based on I^- HR-ToF-CIMS measurement, the concentration of isoprene oxidation products, such as IEPOX+ISOPOOH ($C_5H_{10}O_3 \bullet I^-$) and isoprene hydroxyl nitrates ($C_5H_9NO_4 \bullet I^-$), did not change

after α-pinene injection (Fig. S3b). In addition, after injecting α-pinene, the SOA concentration increases less than 4 μg m^{-3}, which does not substantially perturb the gas/particle partition of pre-existing semi-volatile species. Finally, the time series of isoprene-OA and LO-OOA in the same α-pinene perturbation experiment is strongly correlated (Fig. S4a). It is well studied that isoprene produces SOA slower than α-pinene, as isoprene SOA involves higher-generation products. If the enhancement in isoprene-OA factor is due to isoprene oxidation, the enhancement of isoprene-OA is expected to occur later than the enhancement of LO-OOA, but it is not observed in the experiments. Thus, the strong correlation between isoprene-OA and LO-OOA in the same α-pinene perturbation experiment serves as another evidence that the enhancement in isoprene-OA factor is due to interference from newly formed α-pinene SOA, rather than oxidation of isoprene after injecting α-pinene.

The interference of α-pinene SOA on isoprene-OA factor helps to address some uncertainties regarding the isoprene-OA factor in the literature. For example, Liu et al. (2015) compared the mass spectrum of laboratory-derived IEPOX SOA with isoprene-OA factors at some sites. The authors observed stronger correlation for isoprene-OA factors resolved at Borneo (Robinson et al., 2011a) and Amazon (Chen et al., 2015), and weaker correlation at Atlanta, U.S. (Budisulistiorini et al., 2013) and Ontario, Canada (Slowik et al., 2011). As another example, the fraction of measured total IEPOX SOA molecular tracers in isoprene-OA factor highly varies with location, ranging from 26% at Look Rock, TN (Budisulistiorini et al., 2015) to 78% at Centreville, AL (Hu et al., 2015). To address the uncertainties in above two examples, one possible reason is that the isoprene-OA factors resolved at different sites are not purely from IEPOX uptake. Isoprene-OA factors likely have interference from monoterpenes SOA or other sources, but the interference magnitude varies with locations.

While the perturbation experiments clearly point out the possibility that isoprene-OA factor could have interference from α-pinene SOA, two caveats should be kept in mind. First, in this study, the enhancement magnitude of isoprene-OA is ~20% of LO-OOA enhancement (Fig. S5a), but the interference magnitude would vary with locations and seasons. Second, the perturbation experiments simulate a period with increasing α-pinene SOA concentration. The applicability of the conclusions drawn from this specific scenario to general atmosphere with more dynamic variations of OA sources warrants further exploration.

Primary OA factors, i.e., HOA and COA, only show slight increases in 1 or 2 α-pinene experiments, indicating a lack of interference from α-pinene SOA in these factors.

3.2 β-caryophyllene perturbation experiments

A total of 6 β-caryophyllene perturbation experiments were performed. Initially ~10 ppb β-caryophyllene is injected into the chamber. The concentrations of O_3 and NO_x during β-caryophyllene perturbation experiments are summarized in Table S4. In all β-caryophyllene perturbation experiments, LO-OOA also shows a significant enhancement (Fig. 4b). This clearly shows that the freshly formed SOA from β-caryophyllene oxidation can be another source of LO-OOA. In addition to LO-OOA, COA shows an unexpected increase in 5 out of 6 β-caryophyllene experiments. We have ample evidence that the COA factor at the measurement site has contributions from cooking activities. Firstly, the diurnal variation of COA peaks during meal times (Fig. S6a). Additionally, the COA concentration shows clear increase on football days, consistent with barbecue activities on campus and close to the measurement site. Finally, the COA concentration is enhanced on the days right before the start of a new semester when there are many fraternity/sorority rush events (i.e., barbecue activities) on campus (Fig. S6b and S6c). However, the COA enhancement in β-caryophyllene experiments underscores the fact that COA may not be purely from cooking activities in areas with large biogenic emissions.

3.3 Perturbation experiments with other VOCs

In addition to α-pinene and β-caryophyllene, we also performed a few perturbation experiments by injecting isoprene, *m*-xylene, or naphthalene. However, the SOA formation from these VOCs is not detectable. This is mainly due to either lower SOA yields (of isoprene) or slower oxidation rates (of *m*-xylene and naphthalene) compared to α-pinene and β-caryophyllene, which are discussed in section S6 of Supplement.

We have also performed four perturbation experiments by injecting acidic sulfate particles to probe reactive uptake of IEPOX. We observed enhancement in isoprene-OA concentration after the injection of sulfate particles. The detailed results are included in Appendix B.

3.4 Compare conclusions from lab-in-the-field perturbation experimental approach vs. mass spectra comparison approach

Based on the lab-in-the-field perturbation experiments, we show that fresh SOA from α-pinene and β-caryophyllene oxidations are mainly apportioned into LO-OOA. This finding is consistent with previous studies which concluded that LO-OOA (also denoted as semi-volatile oxygenated organic aerosol, SV-OOA, in older studies) represents freshly formed SOA. The conclusion from previous studies is mainly based on mass spectra comparison approach, that is, the mass spectra of laboratory-generated fresh SOA from various sources are similar to that of LO-OOA (Jimenez et al., 2009; Ng et al., 2010; Marcolli et al., 2006; Kiendler-Scharr et al., 2009). While we acknowledge that the mass spectra comparison approach largely improves our understanding of OA factors, we believe that the perturbation experimental approach provides more objective and quantitative conclusions by addressing some limitations of the mass spectra comparison approach. The mass spectra comparison approach has the following limitations. Firstly, the similarity between two mass spectra is a subjective determination. In other words, what correlation coefficient (R) value implies SOA from a certain source contributes to a specific OA factor? For example, the R values between laboratory generated α-pinene SOA (using HONO as OH source) with LO-OOA, isoprene-OA, and MO-OOA in this study are 0.96, 0.88, and 0.81, respectively. Using these R values to imply whether α-pinene SOA contributes to a certain OA factor or not is subjective. As another example, Jimenez et al. (2009) showed that the mass spectrum of α-pinene SOA becomes more similar to that of MO-OOA than that of LO-OOA with photochemical aging. The ability to determine when and how much α-pinene SOA is apportioned to MO-OOA based on an R value is subjective. Secondly, the conclusions from mass spectra comparison approach are qualitative. Even if the mass spectrum of α-pinene SOA is the most similar to LO-OOA, this similarity does not guarantee that all α-pinene SOA is apportioned into LO-OOA and this similarity does not provide information regarding what fraction of α-pinene SOA is apportioned into LO-OOA.

The perturbation experiments could address the limitations of mass spectra comparison approach and provide more objective and quantitative conclusions. Firstly, the perturbation experiments simulate a short period of time with increasing α-pinene SOA concentration. We perform PMF analysis on the combined ambient data and perturbation data. PMF analysis does not distinguish SOA from natural α-pinene vs. from injected α-pinene, so that PMF analysis can objectively apportion α-pinene SOA into factors. Thus, the conclusions from the perturbation experiments are directly drawn without any subjective judgement on the similarity in mass spectra.

Secondly, using the perturbation data, we attempt to quantify the fraction of fresh α-pinene SOA that is apportioned into different factors (i.e., ~80% into LO-OOA, ~20% into isoprene-OA, 0% into MO-OOA, COA, and HOA). Although further studies are required to extrapolate the conclusions from perturbation experiments to real atmosphere, a similar quantitative understanding cannot be obtained from simple mass spectra comparison approach. Thirdly, the perturbation experiments have the potential to utilize subtle differences across the entire the mass spectrum to evaluate the sources of OA factors. Based on previous laboratory study, the mass spectrum of α-pinene SOA is highly correlated (R = 0.97) with that of β-caryophyllene SOA (Bahreini et al., 2005). Using a mass spectra comparison approach would suggest that these mass spectra are too similar to be differentiated by PMF analysis. However, perturbation experiments show different behaviors of α-pinene SOA and β-caryophyllene SOA. That is, a fraction of the fresh β-caryophyllene SOA is apportioned into COA factor, but similar behavior is not observed for α-pinene SOA. The different behaviors are likely due to the subtle differences in their mass spectra. For example, f_{55} (i.e., the ratio of *m/z* 55 to total signal in the mass spectrum) is typically higher in β-caryophyllene SOA than α-pinene SOA (Bahreini et al., 2005; Tasoglou and Pandis, 2015), and the mass spectrum of COA is characterized by prominent signal at *m/z* 55 (Fig. 2). Overall, the perturbation experiments provide more objective and quantitative insights into the sources of OA factors than traditional mass spectra comparison approach.

3.5 LO-OOA as a surrogate of SOA_{MT+SQT} in the Southeastern U.S.

We propose that the major source of LO-OOA in the southeastern U.S. is the fresh SOA from oxidation of MT and SQT by various oxidants (O_3, OH, and NO_3), based on the following piece of evidence. First, the southeastern U.S. is characterized by large biogenic emissions, including monoterpenes and sesquiterpenes (Guenther et al., 2012). Second, the majority of carbon in SOA is modern in the southeastern U.S. Weber et al. (2007) measured that the biogenic fraction of SOA is roughly 70-80% at two urban sites in Georgia that were also used in our study. We note that measurements in Weber et al. (2007) were performed in 2004 and the biogenic fraction of SOA is expected to be higher in 2016 than 2004, as a result of reductions in anthropogenic emissions (Blanchard et al., 2010). Third, previous studies suggest that the oxidation of β-pinene (another important monoterpene) by nitrate radicals (NO_3) contributes to LO-OOA in the southeastern U.S. (Boyd et al., 2015; Xu et al., 2015a), though this reaction alone cannot replicate the magnitude of LO-OOA (Pye et al., 2015). Fourth, the mass spectra of LO-OOA are almost identical (i.e., R

ranges from 0.95 to 0.99 in Fig. S7) across all the seven datasets in our study. In addition, LO-OOA across all datasets also shares the same diurnal trends (Xu et al., 2015a). The similarity in LO-OOA features suggests that LO-OOA generally share similar sources across multiple sites and in different seasons in the southeastern U.S. Fifth, the lab-in-the-field perturbation experiments provide objective evidence that the majority of freshly formed SOA from the oxidation of MT and SQT contributes to LO-OOA. Sixthly, using the updated CMAQ model (i.e., explicit organic nitrates and Saha and Grieshop (2016) VBS for MT+O_3/OH SOA), we found that the simulated SOA_{MT+SQT} reasonably reproduces both the magnitude and diurnal variability of LO-OOA for all sites (Fig. 6a). The model bias is within ~20% for most sites, except for Centreville, Alabama (i.e., 43% for CTR_June dataset). Fig. 6b present maps of ground-level SOA_{MT+SQT} concentration corresponding to the time periods of observational data, and the SOA_{MT+SQT} concentration is substantially higher in the southeast than other U.S. regions. While, the SOA_{MT+SQT} is present throughout the year, it reaches the largest concentration in summer. The spatial and seasonal variation of SOA_{MT+SQT} concentration is consistent with MT and SQT emissions (Guenther et al., 2012). The consistency between modeled SOA_{MT+SQT} and measured LO-OOA at multiple sites and in different seasons builds confidence in our hypothesis that LO-OOA largely arises from the oxidation of MT and SQT in the southeastern U.S.

We note that we do not conclude that LO-OOA arises exclusively from MT and SQT. SOA from other precursors or other pathways may contribute to LO-OOA, but the related contributions are expected to be much smaller than MT and SQT in the southeastern U.S. Firstly, the contributions of anthropogenic SOA to LO-OOA are likely small. The emissions of anthropogenic VOCs are much weaker than that of biogenic VOCs in the southeastern U.S. (Goldstein et al., 2009). We modeled that the concentration of anthropogenic SOA is on the order of 0.1 $\mu g\ m^{-3}$ for our datasets (Fig. S8). Even if we double the SOA yields of anthropogenic VOCs to account for the potential vapor wall loss in laboratory studies (Zhang et al., 2014), the concentration of SOA from anthropogenic VOCs oxidation is still negligible compared to SOA_{MT+SQT}. The low modeled concentration of anthropogenic SOA is consistent with Zhang et al. (2018), who showed that the measured tracers of anthropogenic SOA only account for 2% of total OA in Centreville, AL. Secondly, other reaction pathways, like aqueous-phase chemistry or some unexplored reaction, may contribute to LO-OOA. However, the consistency between modeled SOA_{MT+SQT} and LO-OOA suggests that LO-OOA can be reasonably represented by a model based on current

knowledge and it is not necessary to invoke any unexplored mechanisms. In addition, SOA produced from aqueous-phase chemistry is generally highly oxidized (Lee et al., 2011) and may be apportioned into MO-OOA, instead of LO-OOA. A recent study by Xu et al. (2016c) suggests that aqueous-phase SOA is a major source of MO-OOA in China.

We limit our hypothesis that major source of LO-OOA is the oxidation of MT and SQT to the southeastern U.S. There is clear evidence that LO-OOA factor represents different sources at different locations. For example, radiocarbon analysis shows that 68-75% of carbon in LO-OOA in California stems from fossil sources (Hayes et al., 2013; Zotter et al., 2014), suggesting the contribution from anthropogenic SOA to LO-OOA. Also, in the wintertime of many locations, LO-OOA and MO-OOA are not separated and a single OOA factor is resolved (Xu et al., 2016b; Lanz et al., 2008).

3.6 Connection between laboratory and field studies

Due to the difficulties associated with accurately measuring complex chemical processes in the atmosphere, laboratory studies have been an integral part in our understanding of atmospheric chemistry (Burkholder et al., 2017). However, the representativeness of laboratory studies under simplified conditions with respect to the complex atmosphere is difficult to evaluate. One unique feature of our lab-in-the-field approach is that the VOC oxidation and SOA formation proceed under realistic atmospheric conditions. Taking advantage of this, we provide a direct link between laboratory studies and ambient observations. Previous laboratory studies have shown that NO can affect SOA composition by influencing the fate of organic peroxy radical (RO_2, a critical radical intermediate formed from VOC oxidation) (Kroll and Seinfeld, 2008; Sarrafzadeh et al., 2016; Presto et al., 2005). To evaluate the representativeness of laboratory studies and investigate the effects of NO on SOA composition, in Fig. 7, we compare the chemical composition of α-pinene SOA formed in laboratory studies under different NO conditions (denoted as SOA_{lab}) with those in α-pinene ambient perturbation experiments (denoted as $SOA_{ambient}$). The degree of similarity in OA mass spectra (i.e., evaluated by the correlation coefficient) between laboratory α-pinene SOA generated under NO-free condition (i.e., denoted as $SOA_{lab,NO\text{-}free}$, using H_2O_2 photolysis as oxidant source) and $SOA_{ambient}$ shows a strong dependence on ambient NO concentration, under which the $SOA_{ambient}$ is formed. The degree of similarity in mass spectra decreases rapidly when ambient NO increases from 0.1 to 0.2ppb, and then reaches a plateau at ~0.3ppb NO. The opposite trend is

observed when laboratory α-pinene SOA generated in the presence of high NO concentrations (i.e., denoted as $SOA_{lab,high\text{-}NO}$, using the photolysis of NO_2 or nitrous acid as oxidant source) are compared with $SOA_{ambient}$. These observations show the transition of RO_2 fate as a function of NO under ambient conditions. For the perturbation experiments performed when ambient NO is below ~0.1ppb, the mass spectra of $SOA_{ambient}$ are similar to $SOA_{lab,NO\text{-}free}$, consistent with that RO_2 mainly reacts with hydroperoxyl (HO_2) or isomerizes. In contrast, for the perturbation experiments performed when ambient NO is above ~0.3ppb, the mass spectra of $SOA_{ambient}$ are similar to $SOA_{lab,high\text{-}NO}$, consistent with that the RO_2 fate is dominated by NO. This NO level (~0.3ppb) is consistent with the NO level required to dominate the fate of RO_2 in the atmosphere, as calculated by using previously measured HO_2 and kinetic rate constants (section S8 of Supplement). These observations also illustrate that the SOA composition from laboratory studies can be representative of atmosphere. We note that the mass spectra of $SOA_{ambient}$ are generally more similar with that of laboratory SOA generated using NO_2 photolysis as oxidant source than using nitrous acid photolysis. This suggests that laboratory experiments using NO_2 photolysis as oxidant source better represent ambient high NO oxidation conditions in the southeastern U.S. than experiments using nitrous acid do. Possible explanations are discussed in section S7 of Supplement. This finding provides new insights into designing future laboratory experiments to better mimic the oxidations in ambient environments.

4 Implications

In this study, we performed lab-in-the-field perturbation experiments and provided objective evidence that the majority of fresh SOA from the oxidation of MT and SQT contributes to LO-OOA. Based on weight of evidence, we propose that LO-OOA can be used as a surrogate of fresh SOA from MT and SQT in the southeastern U.S. We showed that modeled SOA_{MT+SQT} could reasonably reproduce both the magnitude and diurnal variability of LO-OOA at different sites and in different seasons. Based on the model simulation, we estimate that the annual concentration of SOA_{MT+SQT} in $PM_{2.5}$ in the southeastern U.S. is ~2.1 $\mu g\ m^{-3}$ (i.e., average concentration over the six sampling periods and over the southeastern U.S. in the updated simulation). This accounts for 21% of World Health Organization $PM_{2.5}$ guideline (i.e., 10 $\mu g\ m^{-3}$ annual mean) and indicates a significant contributor of environmental risk to the 77 million habitants in the southeastern U.S. Also, the estimated abundance of SOA_{MT+SQT} is substantially larger than represented in current models (Lane et al., 2008; Zheng et al., 2015), but in line with the conclusion from Zhang et al.

(2018). Zhang et al. (2018) used a different methodology, characterization of molecular tracers of MT SOA at Centreville, AL (a site included in our study as well), to conclude that monoterpenes are the largest source of summertime organic aerosol in the southeastern United States. The oxidation of MT and SQT is likely an under-estimated contributor to PM in the present day and perhaps during the pre-industrial period, which determines the baseline state of atmosphere and the estimate of climate forcing by anthropogenic emissions (Carslaw et al., 2013). Models need to improve the description of the MT and SQT oxidation to reduce the uncertainties in estimated OA budget and subsequent climate forcing.

Using LO-OOA as a surrogate of SOA_{MT+SQT} in the southeastern U.S., our ambient ground measurements suggest that at least 19-34% of OA in the southeastern U.S. is from the oxidation of biogenic monoterpenes and sesquiterpenes (Xu et al., 2015a). The fraction of biogenic OA in the southeastern U.S. is even larger if we consider that isoprene-OA could account for 21-36% of OA in summer (albeit potential interferences of SOA from monoterpenes oxidation) and that MO-OOA (24-49% of OA) likely contains SOA from long-term photochemical oxidation of biogenic VOCs. The dominant biogenic origin of SOA poses a challenge to control its burden in the southeastern U.S., if the roles of anthropogenic oxidants and other controlling factors are not recognized. Previous studies have shown that the SOA formation from biogenic VOCs can be mediated by anthropogenic emissions, such as nitrogen oxides and sulfur dioxide (Hoyle et al., 2011; Goldstein et al., 2009; Surratt et al., 2010; Rollins et al., 2012; Xu et al., 2015a). Thus, regulating anthropogenic emissions could help reduce SOA concentration (Lane et al., 2008; Pye et al., 2015; Zheng et al., 2015). For example, as observed in our ambient perturbation experiments, one controlling parameter of α-pinene SOA formation is the concentration of atmospheric oxidants (O_3, OH, and NO_3), which are known to strongly depend on NO_x concentration. As it has been shown that anthropogenic emissions exert complex and non-linear influences on biogenic SOA formation (Zheng et al., 2015), the effectiveness of regulating anthropogenic emissions on biogenic SOA burden requires careful investigations.

The lab-in-the-field perturbation experiments provide insights into the OA factors. This experimental approach can be easily adapted. Future experiments conducted under various ambient environments and with diverse SOA precursors would facilitate the understanding of OA factors in other regions of the world.

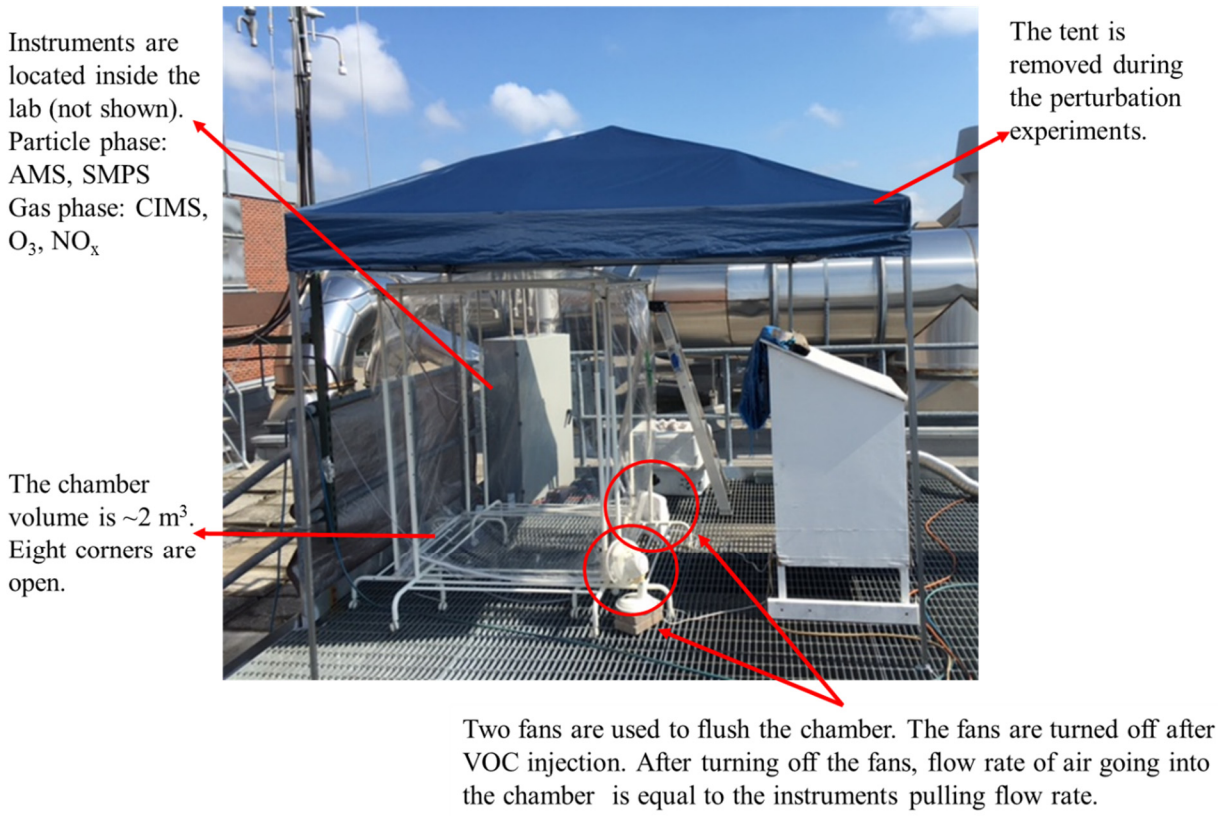

578

579 Fig. 1. The instrument setup for ambient perturbation experiments.

580

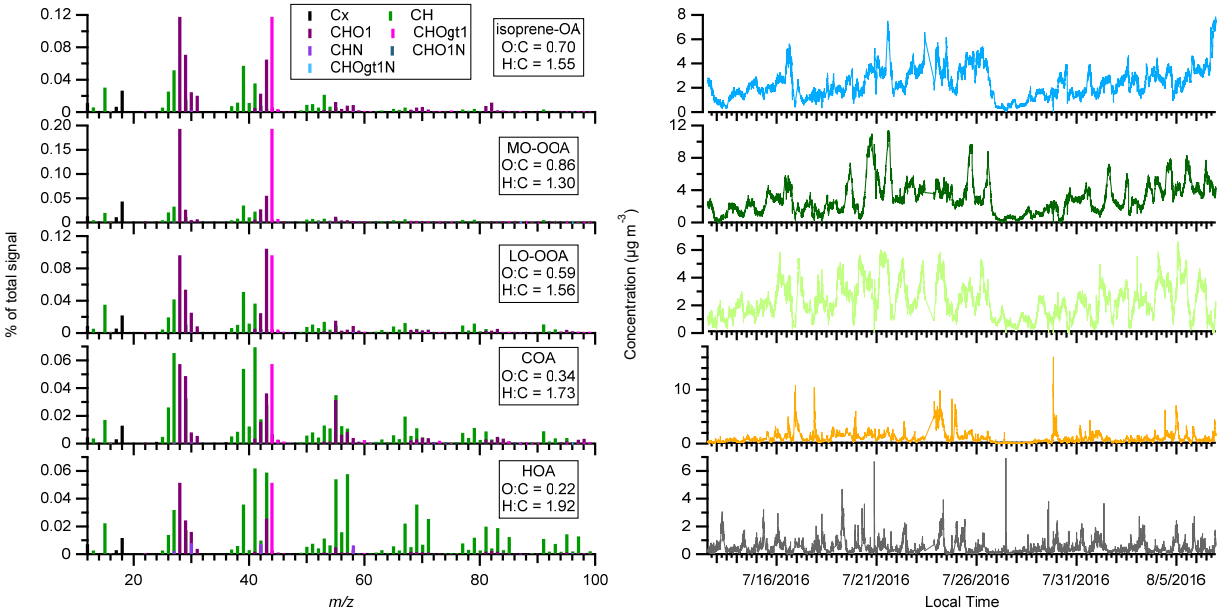

581

582 Fig. 2. The mass spectra and time series of OA factors in perturbation study. The time series
583 includes both the ambient data and perturbation experiments data.

584

585

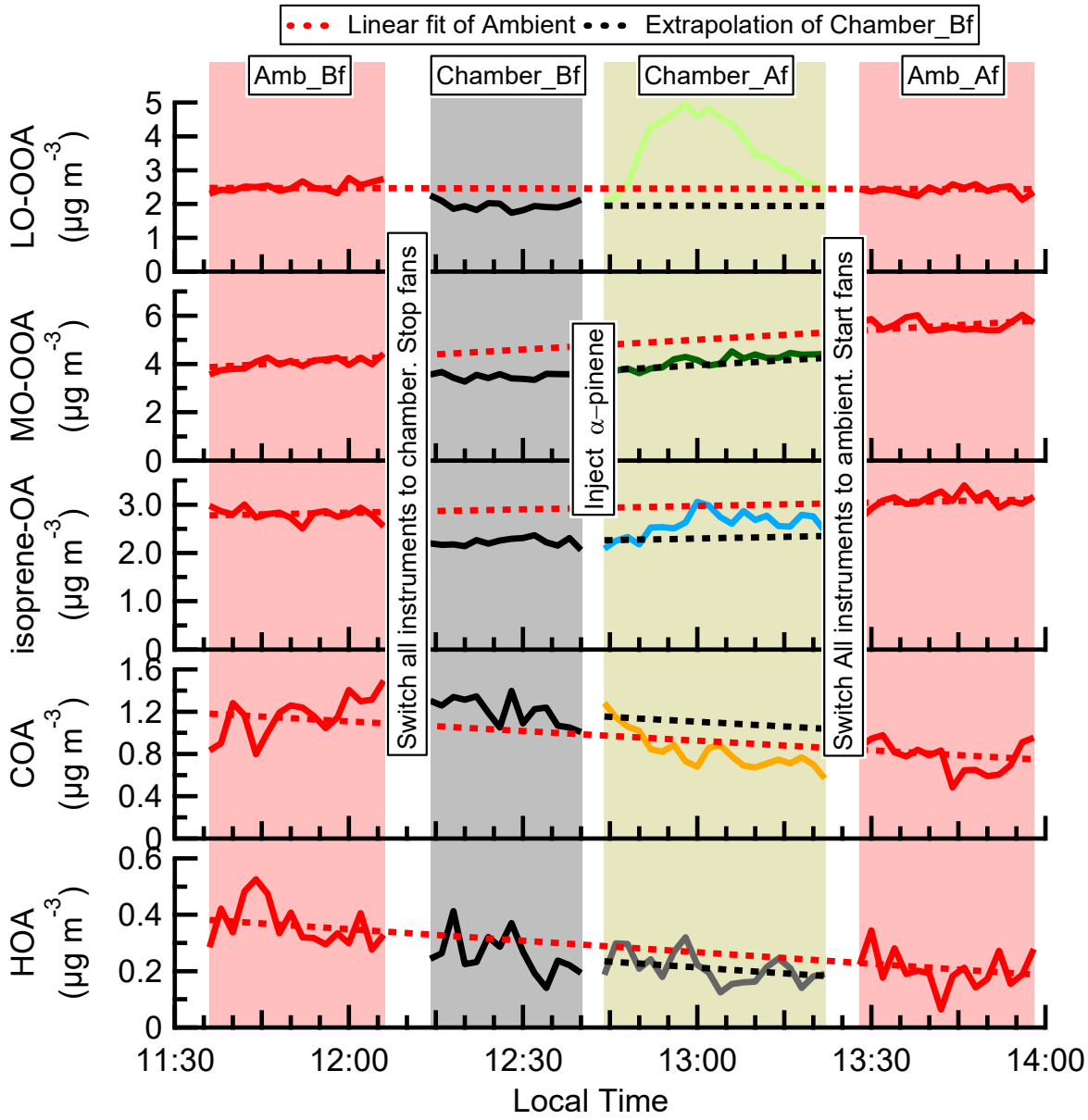

586

587 Fig. 3. The time series of OA factors in an α-pinene perturbation experiment (Expt ID: ap_0801_1).
588 Each perturbation experiment includes four periods: Amb_Bf (~30min), Chamber_Bf (~30min),
589 Chamber_Af (~40min), and Amb_Af (~40min). "Amb" and "Chamber" represent that instruments
590 are sampling ambient and chamber, respectively. "Bf" and "Af" stand for before and after
591 perturbation, respectively. The solid lines are measurement data. The dashed red lines are the linear
592 fits of ambient data (i.e., combined Amb_Bf and Amb_Af). The slopes are used to extrapolate
593 Chamber_Bf data to Chamber_Af period (i.e., dashed black lines). The validity of the linearity
594 assumption is discussed in Appendix A. The difference between measurements (i.e., solid lines)
595 and extrapolated Chamber_Bf (i.e., dashed black lines) represents the change caused by
596 perturbation.

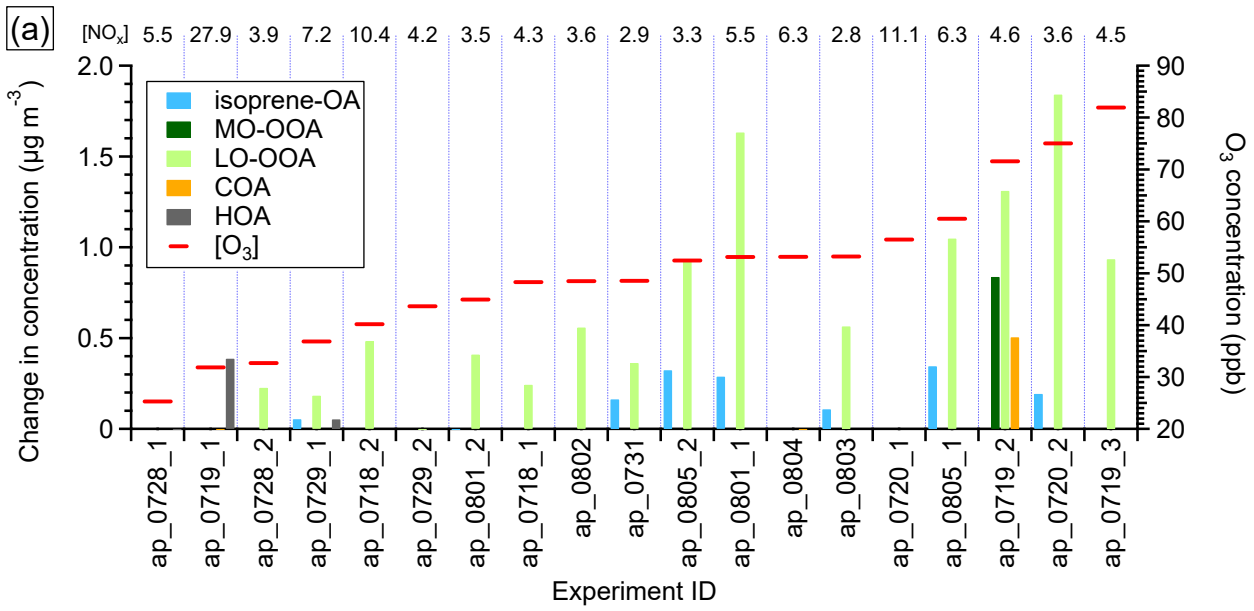

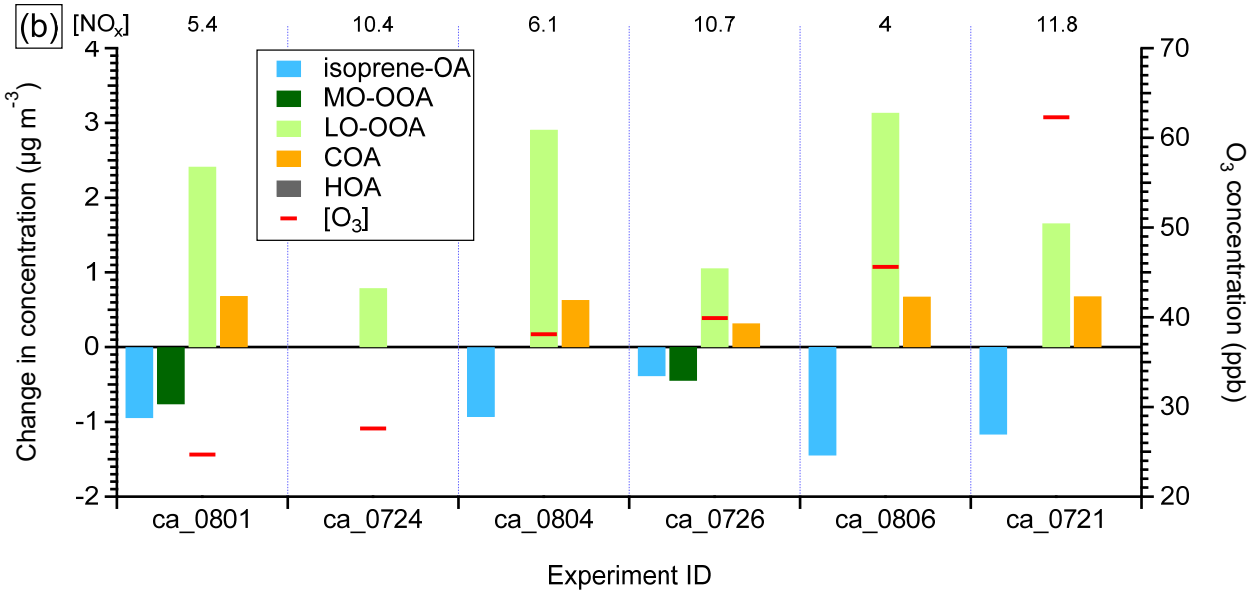

Fig. 4. The statistically significant changes in the concentrations of OA factors after perturbation by (a) α-pinene and (b) β-caryophyllene. The experiments are sorted by average [O_3] during Chamber_Af. The average [NO_x] during Chamber_Af are shown on top of the figure. The changes in concentration are the differences between measurements during Chamber_Af and extrapolated Chamber_Bf (Appendix A). A set of criteria are developed to evaluate if the changes are statistically significant and if the changes are due to ambient variation (Appendix A). Isoprene-OA decreases after β-caryophyllene injection. The reason for this decrease is unclear, but likely due to the limitations of PMF analysis, which assumes constant mass spectra of OA factors over time (section S3 of Supplement).

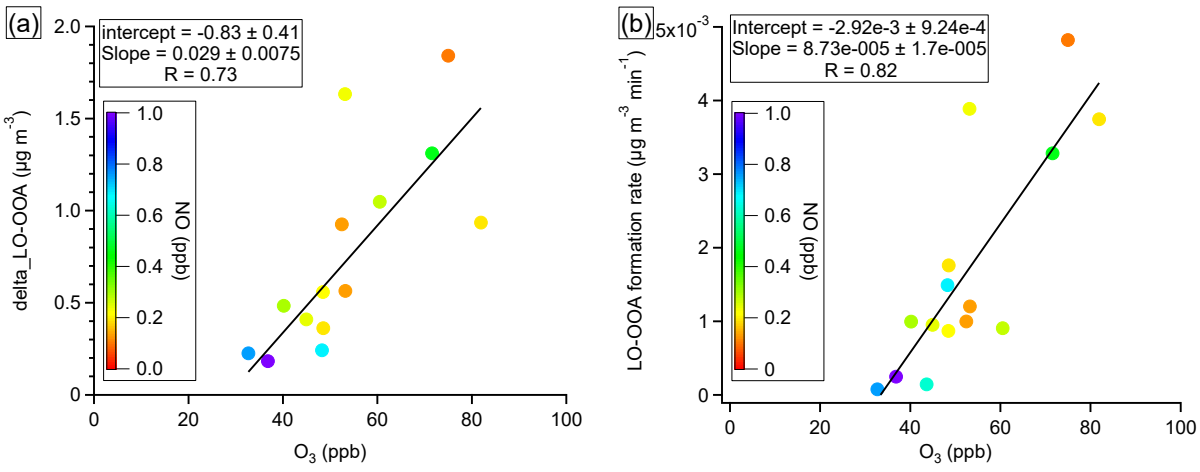

608

609 Fig. 5. Observations of trends in (a) LO-OOA enhancement amount and (b) LO-OOA formation
610 rate with O_3 concentration in α-pinene perturbation experiments. The data points are colored by
611 average NO concentration during Chamber_Af period. The slopes, intercepts, and correlation
612 coefficients (R) are obtained by least square fit.

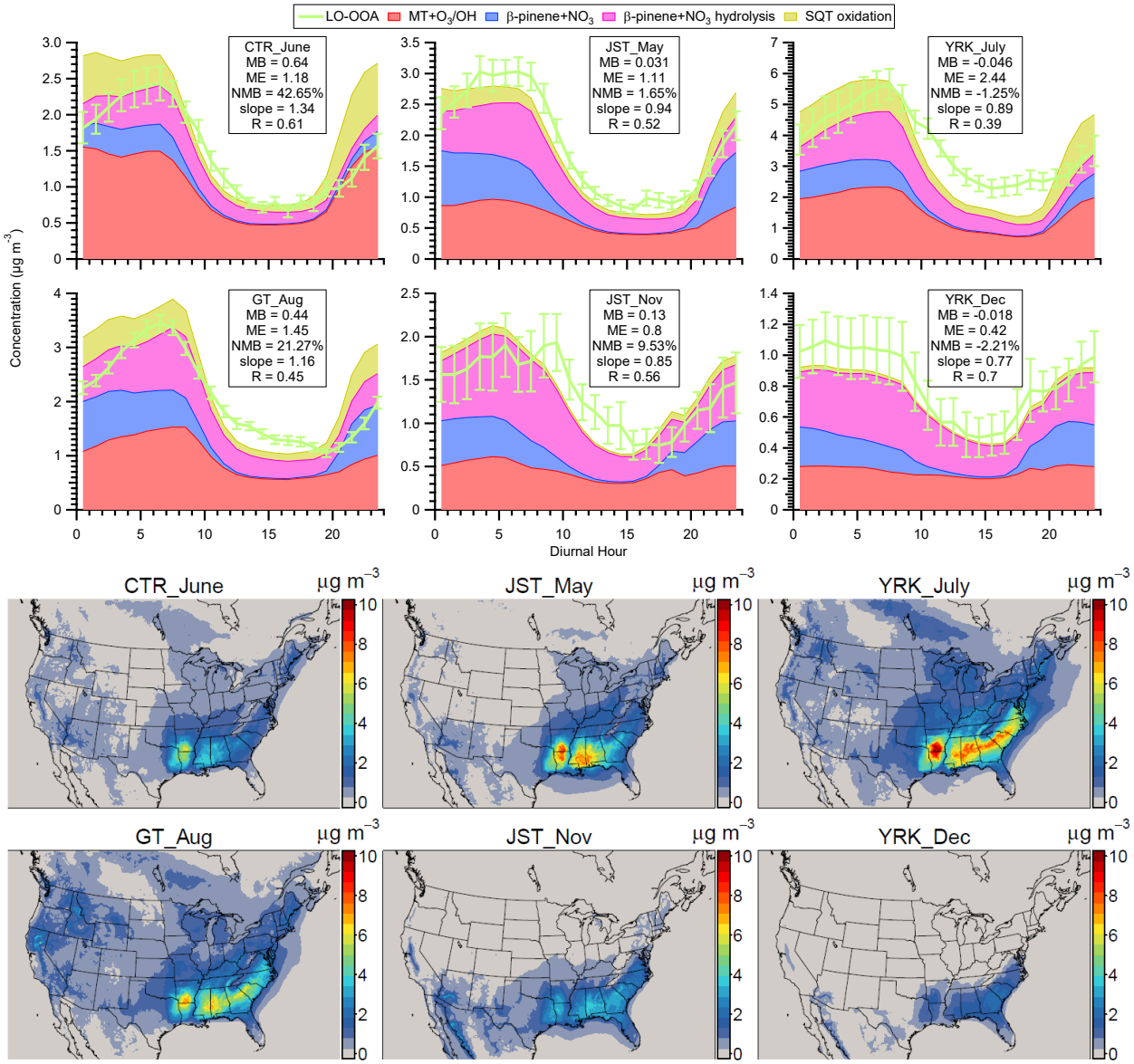

Fig. 6. (a) top panel: the diurnal trends of LO-OOA and modeled SOA from monoterpenes and sesquiterpenes (SOA_{MT+SQT}) at different sampling sites in the southeastern U.S. (b) bottom panel: maps of modeled ground-level SOA_{MT+SQT} concentration coinciding with the time periods of intensive ambient sampling. Model results shown here are from the updated simulation. Abbreviations correspond to Centreville (CTR), Jefferson Street (JST), Yorkville (YRK), Georgia Institute of Technology (GT). Detailed sampling periods are shown in Table S1. In panel (a), since the perturbation experiments show that 16% of SOA from α-pinene oxidation is apportioned into isoprene-OA (Fig. S5a), we only include 84% of modeled SOA from $MT+O_3/OH$ when comparing with LO-OOA for the sites with isoprene-OA. The mean bias (MB), mean error (ME), and normalized mean bias (NMB) for each site are shown in each panel. The slopes and correlation coefficients (R) are obtained by least square fit. The error bars indicate the standard error. In panel (b), average SOA_{MT+SQT} concentration in $PM_{2.5}$ during each sampling period is reported.

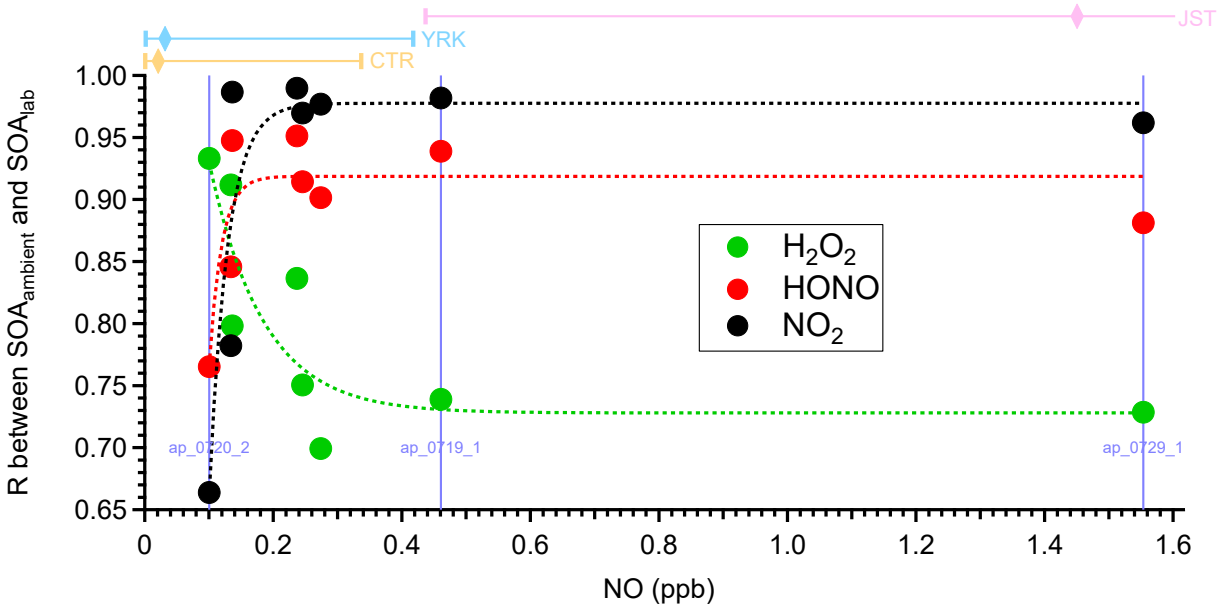

Fig. 7. The correlation coefficients between the mass spectra of OA formed in laboratory under different NO conditions ("SOA_{lab}") and those of OA formed in ambient α-pinene perturbation experiments ("$SOA_{ambient}$"). The subscripts "$_{lab}$" and "$_{ambient}$" indicate the SOA formed under laboratory conditions and ambient conditions, respectively. Three different oxidant sources (i.e., H_2O_2, HONO, and NO_2) are used to create different NO concentrations in laboratory studies. The mass spectra of "$SOA_{ambient}$" are calculated by comparing the mass spectra of OA during Chamber_Af and those of extrapolated Chamber_Bf (section S7 of Supplement). To calculate reliable mass spectra of "$SOA_{ambient}$", only the experiments with significant OA enhancement are analyzed and shown here (Appendix A). The x-axis is the average NO concentration during each perturbation experiment. The data points on the same vertical line (i.e., the same NO concentration) are from the same perturbation experiment, but compared to three different laboratory experiments. The dashed lines are used to guide eyes. The bars on top of the figure represent the 10th, 50th, and 90th percentiles of NO concentration for CTR (Centreville, AL), YRK (Yorkville, GA), and JST (Jefferson Street, GA) in 2013. The NO concentration is measured by the SouthEastern Aerosol Research and Characterization (SEARCH) network. The 90th percentile of NO concentration in JST is 14.8 ppb, which is not shown in the figure.

Acknowledgments

L.X. and N.L.N. acknowledged support from US Environmental Protection Agency (EPA) STAR Grant RD-83540301, and National Science Foundation (NSF) grants 1555034 and 1455588. The HR-ToF-CIMS was purchased with NSF Major Research Instrumentation (MRI) grant 1428738. HOTP contributions were supported by a Presidential Early Career Award for Scientists and Engineers (PECASE). The authors thank R. J. Weber and M. R. Canagaratna for helpful discussions, the SEARCH personnel for their many contributions, the CSRA for preparing emissions and meteorology for CMAQ simulations. The US EPA through its Office of Research and Development supported the research described here. It has been subjected to Agency administrative review and approved for publication but may not necessarily reflect official Agency policy.

References

Allan, J. D., Williams, P. I., Morgan, W. T., Martin, C. L., Flynn, M. J., Lee, J., Nemitz, E., Phillips, G. J., Gallagher, M. W., and Coe, H.: Contributions from transport, solid fuel burning and cooking to primary organic aerosols in two UK cities, Atmos. Chem. Phys., 10, 647-668, 10.5194/acp-10-647-2010, 2010.

Appel, K. W., Napelenok, S. L., Foley, K. M., Pye, H. O. T., Hogrefe, C., Luecken, D. J., Bash, J. O., Roselle, S. J., Pleim, J. E., Foroutan, H., Hutzell, W. T., Pouliot, G. A., Sarwar, G., Fahey, K. M., Gantt, B., Gilliam, R. C., Heath, N. K., Kang, D., Mathur, R., Schwede, D. B., Spero, T. L., Wong, D. C., and Young, J. O.: Description and evaluation of the Community Multiscale Air Quality (CMAQ) modeling system version 5.1, Geosci. Model Dev., 10, 1703-1732, 10.5194/gmd-10-1703-2017, 2017.

Bahreini, R., Keywood, M. D., Ng, N. L., Varutbangkul, V., Gao, S., Flagan, R. C., Seinfeld, J. H., Worsnop, D. R., and Jimenez, J. L.: Measurements of secondary organic aerosol from oxidation of cycloalkenes, terpenes, and m-xylene using an Aerodyne aerosol mass spectrometer, Environ Sci Technol, 39, 5674-5688, Doi 10.1021/Es048061a, 2005.

Beddows, D. C. S., Harrison, R. M., Green, D. C., and Fuller, G. W.: Receptor modelling of both particle composition and size distribution from a background site in London, UK, Atmos. Chem. Phys., 15, 10107-10125, 10.5194/acp-15-10107-2015, 2015.

Blanchard, C. L., Hidy, G. M., Tanenbaum, S., Rasmussen, R., Watkins, R., and Edgerton, E.: NMOC, ozone, and organic aerosol in the southeastern United States, 1999-2007 1 Spatial and temporal variations of NMOC concentrations and composition in Atlanta, Georgia, Atmospheric Environment, 44, 4827-4839, DOI 10.1016/j.atmosenv.2010.08.036, 2010.

Bougiatioti, A., Stavroulas, I., Kostenidou, E., Zarmpas, P., Theodosi, C., Kouvarakis, G., Canonaco, F., Prévôt, A. S. H., Nenes, A., Pandis, S. N., and Mihalopoulos, N.: Processing of biomass-burning aerosol in the eastern Mediterranean during summertime, Atmos. Chem. Phys., 14, 4793-4807, 10.5194/acp-14-4793-2014, 2014.

Boyd, C. M., Sanchez, J., Xu, L., Eugene, A. J., Nah, T., Tuet, W. Y., Guzman, M. I., and Ng, N. L.: Secondary organic aerosol formation from the β-pinene+NO3 system: effect of humidity and peroxy radical fate, Atmos. Chem. Phys., 15, 7497-7522, 10.5194/acp-15-7497-2015, 2015.

Budisulistiorini, S. H., Canagaratna, M. R., Croteau, P. L., Marth, W. J., Baumann, K., Edgerton, E. S., Shaw, S. L., Knipping, E. M., Worsnop, D. R., Jayne, J. T., Gold, A., and Surratt, J. D.: Real-Time Continuous Characterization of Secondary Organic Aerosol Derived from Isoprene Epoxydiols in Downtown Atlanta, Georgia, Using the Aerodyne Aerosol Chemical Speciation Monitor, Environ Sci Technol, 47, 5686-5694, Doi 10.1021/Es400023n, 2013.

Budisulistiorini, S. H., Li, X., Bairai, S. T., Renfro, J., Liu, Y., Liu, Y. J., McKinney, K. A., Martin, S. T., McNeill, V. F., Pye, H. O. T., Nenes, A., Neff, M. E., Stone, E. A., Mueller, S., Knote, C., Shaw, S. L., Zhang, Z., Gold, A., and Surratt, J. D.: Examining the effects of anthropogenic emissions on isoprene-derived secondary organic aerosol formation during the 2013 Southern Oxidant and Aerosol Study (SOAS) at the Look Rock, Tennessee ground site, Atmos. Chem. Phys., 15, 8871-8888, 10.5194/acp-15-8871-2015, 2015.

Burkholder, J. B., Abbatt, J. P. D., Barnes, I., Roberts, J. M., Melamed, M. L., Ammann, M., Bertram, A. K., Cappa, C. D., Carlton, A. M. G., Carpenter, L. J., Crowley, J. N., Dubowski, Y., George, C., Heard, D. E., Herrmann, H., Keutsch, F. N., Kroll, J. H., McNeill, V. F., Ng, N. L., Nizkorodov, S. A., Orlando, J. J., Percival, C. J., Picquet-Varrault, B., Rudich, Y., Seakins, P. W., Surratt, J. D., Tanimoto, H., Thornton, J. A., Zhu, T., Tyndall, G. S., Wahner, A., Weschler, C. J., Wilson, K. R., and Ziemann, P. J.: The Essential Role for Laboratory Studies in Atmospheric Chemistry, Environ Sci Technol, 10.1021/acs.est.6b04947, 2017.

Canagaratna, M. R., Jayne, J. T., Jimenez, J. L., Allan, J. D., Alfarra, M. R., Zhang, Q., Onasch, T. B., Drewnick, F., Coe, H., Middlebrook, A., Delia, A., Williams, L. R., Trimborn, A. M., Northway, M. J., DeCarlo, P. F., Kolb, C. E., Davidovits, P., and Worsnop, D. R.: Chemical and microphysical characterization of ambient aerosols with the aerodyne aerosol mass spectrometer, Mass Spectrometry Reviews, 26, 185-222, 10.1002/mas.20115, 2007.

Canonaco, F., Crippa, M., Slowik, J. G., Baltensperger, U., and Prévôt, A. S. H.: SoFi, an IGOR-based interface for the efficient use of the generalized multilinear engine (ME-2) for the source apportionment: ME-2 application to aerosol mass spectrometer data, Atmos. Meas. Tech., 6, 3649-3661, 10.5194/amt-6-3649-2013, 2013.

Carlton, A. G., Bhave, P. V., Napelenok, S. L., Edney, E. O., Sarwar, G., Pinder, R. W., Pouliot, G. A., and Houyoux, M.: Model Representation of Secondary Organic Aerosol in CMAQv4.7, Environ Sci Technol, 44, 8553-8560, 10.1021/es100636q, 2010.

Carslaw, K. S., Lee, L. A., Reddington, C. L., Pringle, K. J., Rap, A., Forster, P. M., Mann, G. W., Spracklen, D. V., Woodhouse, M. T., Regayre, L. A., and Pierce, J. R.: Large contribution of natural aerosols to uncertainty in indirect forcing, Nature, 503, 67-71, Doi 10.1038/Nature12674, 2013.

Chen, Q., Farmer, D. K., Rizzo, L. V., Pauliquevis, T., Kuwata, M., Karl, T. G., Guenther, A., Allan, J. D., Coe, H., Andreae, M. O., Pöschl, U., Jimenez, J. L., Artaxo, P., and Martin, S. T.: Submicron particle mass concentrations and sources in the Amazonian wet season (AMAZE-08), Atmos. Chem. Phys., 15, 3687-3701, 10.5194/acp-15-3687-2015, 2015.

Crippa, M., Canonaco, F., Lanz, V. A., Äijälä, M., Allan, J. D., Carbone, S., Capes, G., Ceburnis, D., Dall'Osto, M., Day, D. A., DeCarlo, P. F., Ehn, M., Eriksson, A., Freney, E., Hildebrandt Ruiz, L., Hillamo, R., Jimenez, J. L., Junninen, H., Kiendler-Scharr, A., Kortelainen, A. M., Kulmala,

743 M., Laaksonen, A., Mensah, A. A., Mohr, C., Nemitz, E., O'Dowd, C., Ovadnevaite, J., Pandis, S.
744 N., Petäjä, T., Poulain, L., Saarikoski, S., Sellegri, K., Swietlicki, E., Tiitta, P., Worsnop, D. R.,
745 Baltensperger, U., and Prévôt, A. S. H.: Organic aerosol components derived from 25 AMS data
746 sets across Europe using a consistent ME-2 based source apportionment approach, Atmos. Chem.
747 Phys., 14, 6159-6176, 10.5194/acp-14-6159-2014, 2014.
748
749 DeCarlo, P. F., Kimmel, J. R., Trimborn, A., Northway, M. J., Jayne, J. T., Aiken, A. C., Gonin,
750 M., Fuhrer, K., Horvath, T., Docherty, K. S., Worsnop, D. R., and Jimenez, J. L.: Field-Deployable,
751 High-Resolution, Time-of-Flight Aerosol Mass Spectrometer, Anal Chem, 78, 8281-8289,
752 10.1021/ac061249n, 2006.
753
754 Eddingsaas, N. C., Loza, C. L., Yee, L. D., Chan, M., Schilling, K. A., Chhabra, P. S., Seinfeld, J.
755 H., and Wennberg, P. O.: α-pinene photooxidation under controlled chemical conditions –
756 Part 2: SOA yield and composition in low- and high-NOx environments, Atmos. Chem. Phys., 12,
757 7413-7427, 10.5194/acp-12-7413-2012, 2012a.
758
759 Eddingsaas, N. C., Loza, C. L., Yee, L. D., Seinfeld, J. H., and Wennberg, P. O.: α-pinene
760 photooxidation under controlled chemical conditions – Part 1: Gas-phase composition in low- and
761 high-NO_x environments, Atmos. Chem. Phys., 12, 6489-6504, 10.5194/acp-12-
762 6489-2012, 2012b.
763
764 Ehn, M., Thornton, J. A., Kleist, E., Sipila, M., Junninen, H., Pullinen, I., Springer, M., Rubach,
765 F., Tillmann, R., Lee, B., Lopez-Hilfiker, F., Andres, S., Acir, I.-H., Rissanen, M., Jokinen, T.,
766 Schobesberger, S., Kangasluoma, J., Kontkanen, J., Nieminen, T., Kurten, T., Nielsen, L. B.,
767 Jorgensen, S., Kjaergaard, H. G., Canagaratna, M., Maso, M. D., Berndt, T., Petaja, T., Wahner,
768 A., Kerminen, V.-M., Kulmala, M., Worsnop, D. R., Wildt, J., and Mentel, T. F.: A large source
769 of low-volatility secondary organic aerosol, Nature, 506, 476-479, 10.1038/nature13032, 2014.
770
771 El Haddad, I., D'Anna, B., Temime-Roussel, B., Nicolas, M., Boreave, A., Favez, O., Voisin, D.,
772 Sciare, J., George, C., Jaffrezo, J. L., Wortham, H., and Marchand, N.: Towards a better
773 understanding of the origins, chemical composition and aging of oxygenated organic aerosols: case
774 study of a Mediterranean industrialized environment, Marseille, Atmos. Chem. Phys., 13, 7875-
775 7894, 10.5194/acp-13-7875-2013, 2013.
776
777 Goldstein, A. H., Koven, C. D., Heald, C. L., and Fung, I. Y.: Biogenic carbon and anthropogenic
778 pollutants combine to form a cooling haze over the southeastern United States, Proceedings of the
779 National Academy of Sciences, 106, 8835-8840, 10.1073/pnas.0904128106, 2009.
780
781 Grieshop, A. P., Donahue, N. M., and Robinson, A. L.: Laboratory investigation of photochemical
782 oxidation of organic aerosol from wood fires 2: analysis of aerosol mass spectrometer data, Atmos.
783 Chem. Phys., 9, 2227-2240, 10.5194/acp-9-2227-2009, 2009.
784

785 Griffin, R. J., Cocker, D. R., Flagan, R. C., and Seinfeld, J. H.: Organic aerosol formation from
786 the oxidation of biogenic hydrocarbons, J Geophys Res-Atmos, 104, 3555-3567, Doi
787 10.1029/1998jd100049, 1999.
788
789 Guenther, A., Jiang, X., Heald, C. L., Sakulyanontvittaya, T., Duhl, T., Emmons, L. K., and Wang,
790 X.: The Model of Emissions of Gases and Aerosols from Nature version 2.1 (MEGAN2.1): an
791 extended and updated framework for modeling biogenic emissions, Geosci. Model Dev., 5, 1471-
792 1492, 10.5194/gmd-5-1471-2012, 2012.
793
794 Hallquist, M., Wenger, J. C., Baltensperger, U., Rudich, Y., Simpson, D., Claeys, M., Dommen,
795 J., Donahue, N. M., George, C., Goldstein, A. H., Hamilton, J. F., Herrmann, H., Hoffmann, T.,
796 Iinuma, Y., Jang, M., Jenkin, M. E., Jimenez, J. L., Kiendler-Scharr, A., Maenhaut, W., McFiggans,
797 G., Mentel, T. F., Monod, A., Prevot, A. S. H., Seinfeld, J. H., Surratt, J. D., Szmigielski, R., and
798 Wildt, J.: The formation, properties and impact of secondary organic aerosol: current and emerging
799 issues, Atmos Chem Phys, 9, 5155-5236, 2009.
800
801 Hayes, P. L., Ortega, A. M., Cubison, M. J., Froyd, K. D., Zhao, Y., Cliff, S. S., Hu, W. W.,
802 Toohey, D. W., Flynn, J. H., Lefer, B. L., Grossberg, N., Alvarez, S., Rappenglueck, B., Taylor, J.
803 W., Allan, J. D., Holloway, J. S., Gilman, J. B., Kuster, W. C., De Gouw, J. A., Massoli, P., Zhang,
804 X., Liu, J., Weber, R. J., Corrigan, A. L., Russell, L. M., Isaacman, G., Worton, D. R., Kreisberg,
805 N. M., Goldstein, A. H., Thalman, R., Waxman, E. M., Volkamer, R., Lin, Y. H., Surratt, J. D.,
806 Kleindienst, T. E., Offenberg, J. H., Dusanter, S., Griffith, S., Stevens, P. S., Brioude, J., Angevine,
807 W. M., and Jimenez, J. L.: Organic aerosol composition and sources in Pasadena, California,
808 during the 2010 CalNex campaign, J Geophys Res-Atmos, 118, 9233-9257, Doi
809 10.1002/Jgrd.50530, 2013.
810
811 Heath, N. K., Pleim, J. E., Gilliam, R. C., and Kang, D.: A simple lightning assimilation technique
812 for improving retrospective WRF simulations, Journal of Advances in Modeling Earth Systems, 8,
813 1806-1824, 10.1002/2016MS000735, 2016.
814
815 Helmig, D., Ortega, J., Duhl, T., Tanner, D., Guenther, A., Harley, P., Wiedinmyer, C., Milford,
816 J., and Sakulyanontvittaya, T.: Sesquiterpene Emissions from Pine Trees − Identifications,
817 Emission Rates and Flux Estimates for the Contiguous United States, Environ Sci Technol, 41,
818 1545-1553, 10.1021/es0618907, 2007.
819
820 Hennigan, C. J., Bergin, M. H., Russell, A. G., Nenes, A., and Weber, R. J.: Gas/particle
821 partitioning of water-soluble organic aerosol in Atlanta, Atmos Chem Phys, 9, 3613-3628, 2009.
822
823 Hodzic, A., Kasibhatla, P. S., Jo, D. S., Cappa, C. D., Jimenez, J. L., Madronich, S., and Park, R.
824 J.: Rethinking the global secondary organic aerosol (SOA) budget: stronger production, faster
825 removal, shorter lifetime, Atmos. Chem. Phys., 16, 7917-7941, 10.5194/acp-16-7917-2016, 2016.
826

827 Hoyle, C. R., Boy, M., Donahue, N. M., Fry, J. L., Glasius, M., Guenther, A., Hallar, A. G., Hartz,
828 K. H., Petters, M. D., Petaja, T., Rosenoern, T., and Sullivan, A. P.: A review of the anthropogenic
829 influence on biogenic secondary organic aerosol, Atmos Chem Phys, 11, 321-343, DOI
830 10.5194/acp-11-321-2011, 2011.
831
832 Hu, W. W., Campuzano-Jost, P., Palm, B. B., Day, D. A., Ortega, A. M., Hayes, P. L., Krechmer,
833 J. E., Chen, Q., Kuwata, M., Liu, Y. J., de Sá, S. S., McKinney, K., Martin, S. T., Hu, M.,
834 Budisulistiorini, S. H., Riva, M., Surratt, J. D., St. Clair, J. M., Isaacman-Van Wertz, G., Yee, L.
835 D., Goldstein, A. H., Carbone, S., Brito, J., Artaxo, P., de Gouw, J. A., Koss, A., Wisthaler, A.,
836 Mikoviny, T., Karl, T., Kaser, L., Jud, W., Hansel, A., Docherty, K. S., Alexander, M. L., Robinson,
837 N. H., Coe, H., Allan, J. D., Canagaratna, M. R., Paulot, F., and Jimenez, J. L.: Characterization
838 of a real-time tracer for isoprene epoxydiols-derived secondary organic aerosol (IEPOX-SOA)
839 from aerosol mass spectrometer measurements, Atmos. Chem. Phys., 15, 11807-11833,
840 10.5194/acp-15-11807-2015, 2015.
841
842 Huang, X. F., He, L. Y., Hu, M., Canagaratna, M. R., Sun, Y., Zhang, Q., Zhu, T., Xue, L., Zeng,
843 L. W., Liu, X. G., Zhang, Y. H., Jayne, J. T., Ng, N. L., and Worsnop, D. R.: Highly time-resolved
844 chemical characterization of atmospheric submicron particles during 2008 Beijing Olympic
845 Games using an Aerodyne High-Resolution Aerosol Mass Spectrometer, Atmos Chem Phys, 10,
846 8933-8945, DOI 10.5194/acp-10-8933-2010, 2010.
847
848 Jimenez, J. L., Canagaratna, M. R., Donahue, N. M., Prevot, A. S. H., Zhang, Q., Kroll, J. H.,
849 DeCarlo, P. F., Allan, J. D., Coe, H., Ng, N. L., Aiken, A. C., Docherty, K. S., Ulbrich, I. M.,
850 Grieshop, A. P., Robinson, A. L., Duplissy, J., Smith, J. D., Wilson, K. R., Lanz, V. A., Hueglin,
851 C., Sun, Y. L., Tian, J., Laaksonen, A., Raatikainen, T., Rautiainen, J., Vaattovaara, P., Ehn, M.,
852 Kulmala, M., Tomlinson, J. M., Collins, D. R., Cubison, M. J., Dunlea, E. J., Huffman, J. A.,
853 Onasch, T. B., Alfarra, M. R., Williams, P. I., Bower, K., Kondo, Y., Schneider, J., Drewnick, F.,
854 Borrmann, S., Weimer, S., Demerjian, K., Salcedo, D., Cottrell, L., Griffin, R., Takami, A.,
855 Miyoshi, T., Hatakeyama, S., Shimono, A., Sun, J. Y., Zhang, Y. M., Dzepina, K., Kimmel, J. R.,
856 Sueper, D., Jayne, J. T., Herndon, S. C., Trimborn, A. M., Williams, L. R., Wood, E. C.,
857 Middlebrook, A. M., Kolb, C. E., Baltensperger, U., and Worsnop, D. R.: Evolution of Organic
858 Aerosols in the Atmosphere, Science, 326, 1525-1529, DOI 10.1126/science.1180353, 2009.
859
860 Kiendler-Scharr, A., Zhang, Q., Hohaus, T., Kleist, E., Mensah, A., Mentel, T. F., Spindler, C.,
861 Uerlings, R., Tillmann, R., and Wildt, J.: Aerosol Mass Spectrometric Features of Biogenic SOA:
862 Observations from a Plant Chamber and in Rural Atmospheric Environments, Environ Sci Technol,
863 43, 8166-8172, 10.1021/es901420b, 2009.
864
865 Kiendler-Scharr, A., Mensah, A. A., Friese, E., Topping, D., Nemitz, E., Prevot, A. S. H., Äijälä,
866 M., Allan, J., Canonaco, F., Canagaratna, M., Carbone, S., Crippa, M., Dall Osto, M., Day, D. A.,
867 De Carlo, P., Di Marco, C. F., Elbern, H., Eriksson, A., Freney, E., Hao, L., Herrmann, H.,
868 Hildebrandt, L., Hillamo, R., Jimenez, J. L., Laaksonen, A., McFiggans, G., Mohr, C., O'Dowd,
869 C., Otjes, R., Ovadnevaite, J., Pandis, S. N., Poulain, L., Schlag, P., Sellegri, K., Swietlicki, E.,
870 Tiitta, P., Vermeulen, A., Wahner, A., Worsnop, D., and Wu, H. C.: Ubiquity of organic nitrates

from nighttime chemistry in the European submicron aerosol, Geophysical Research Letters, 43, 7735-7744, 10.1002/2016GL069239, 2016.

Kroll, J. H., Ng, N. L., Murphy, S. M., Varutbangkul, V., Flagan, R. C., and Seinfeld, J. H.: Chamber studies of secondary organic aerosol growth by reactive uptake of simple carbonyl compounds, J Geophys Res-Atmos, 110, Doi 10.1029/2005jd006004, 2005.

Kroll, J. H., and Seinfeld, J. H.: Chemistry of secondary organic aerosol: Formation and evolution of low-volatility organics in the atmosphere, Atmospheric Environment, 42, 3593-3624, DOI 10.1016/j.atmosenv.2008.01.003, 2008.

Kurtén, T., Rissanen, M. P., Mackeprang, K., Thornton, J. A., Hyttinen, N., Jørgensen, S., Ehn, M., and Kjaergaard, H. G.: Computational Study of Hydrogen Shifts and Ring-Opening Mechanisms in α-Pinene Ozonolysis Products, The Journal of Physical Chemistry A, 119, 11366-11375, 10.1021/acs.jpca.5b08948, 2015.

Lane, T. E., Donahue, N. M., and Pandis, S. N.: Effect of NOx on Secondary Organic Aerosol Concentrations, Environ Sci Technol, 42, 6022-6027, 10.1021/es703225a, 2008.

Lanz, V. A., Alfarra, M. R., Baltensperger, U., Buchmann, B., Hueglin, C., Szidat, S., Wehrli, M. N., Wacker, L., Weimer, S., Caseiro, A., Puxbaum, H., and Prevot, A. S. H.: Source Attribution of Submicron Organic Aerosols during Wintertime Inversions by Advanced Factor Analysis of Aerosol Mass Spectra, Environ Sci Technol, 42, 214-220, 10.1021/es0707207, 2008.

Lee, A. K. Y., Herckes, P., Leaitch, W. R., Macdonald, A. M., and Abbatt, J. P. D.: Aqueous OH oxidation of ambient organic aerosol and cloud water organics: Formation of highly oxidized products, Geophysical Research Letters, 38, n/a-n/a, 10.1029/2011GL047439, 2011.

Lee, B. H., Lopez-Hilfiker, F. D., Mohr, C., Kurtén, T., Worsnop, D. R., and Thornton, J. A.: An Iodide-Adduct High-Resolution Time-of-Flight Chemical-Ionization Mass Spectrometer: Application to Atmospheric Inorganic and Organic Compounds, Environ Sci Technol, 48, 6309-6317, 10.1021/es500362a, 2014.

Lee, B. H., Mohr, C., Lopez-Hilfiker, F. D., Lutz, A., Hallquist, M., Lee, L., Romer, P., Cohen, R. C., Iyer, S., Kurtén, T., Hu, W., Day, D. A., Campuzano-Jost, P., Jimenez, J. L., Xu, L., Ng, N. L., Guo, H., Weber, R. J., Wild, R. J., Brown, S. S., Koss, A., de Gouw, J., Olson, K., Goldstein, A. H., Seco, R., Kim, S., McAvey, K., Shepson, P. B., Starn, T., Baumann, K., Edgerton, E. S., Liu, J., Shilling, J. E., Miller, D. O., Brune, W., Schobesberger, S., D'Ambro, E. L., and Thornton, J. A.: Highly functionalized organic nitrates in the southeast United States: Contribution to secondary organic aerosol and reactive nitrogen budgets, Proceedings of the National Academy of Sciences, 113, 1516-1521, 10.1073/pnas.1508108113, 2016.

913 Lelieveld, J., Evans, J. S., Fnais, M., Giannadaki, D., and Pozzer, A.: The contribution of outdoor
914 air pollution sources to premature mortality on a global scale, Nature, 525, 367-371,
915 10.1038/nature15371, 2015.
916
917 Leungsakul, S., Jeffries, H. E., and Kamens, R. M.: A kinetic mechanism for predicting secondary
918 aerosol formation from the reactions of d-limonene in the presence of oxides of nitrogen and
919 natural sunlight, Atmospheric Environment, 39, 7063-7082,
920 https://doi.org/10.1016/j.atmosenv.2005.08.024, 2005.
921
922 Liu, Y., Kuwata, M., Strick, B. F., Geiger, F. M., Thomson, R. J., McKinney, K. A., and Martin,
923 S. T.: Uptake of Epoxydiol Isomers Accounts for Half of the Particle-Phase Material Produced
924 from Isoprene Photooxidation via the HO2 Pathway, Environ Sci Technol, 49, 250-258,
925 10.1021/es5034298, 2015.
926
927 Liu, Y., Kuwata, M., McKinney, K. A., and Martin, S. T.: Uptake and release of gaseous species
928 accompanying the reactions of isoprene photo-oxidation products with sulfate particles, Phys
929 Chem Chem Phys, 18, 1595-1600, 10.1039/C5CP04551G, 2016.
930
931 Marcolli, C., Canagaratna, M. R., Worsnop, D. R., Bahreini, R., de Gouw, J. A., Warneke, C.,
932 Goldan, P. D., Kuster, W. C., Williams, E. J., Lerner, B. M., Roberts, J. M., Meagher, J. F.,
933 Fehsenfeld, F. C., Marchewka, M., Bertman, S. B., and Middlebrook, A. M.: Cluster Analysis of
934 the Organic Peaks in Bulk Mass Spectra Obtained During the 2002 New England Air Quality
935 Study with an Aerodyne Aerosol Mass Spectrometer, Atmos. Chem. Phys., 6, 5649-5666,
936 10.5194/acp-6-5649-2006, 2006.
937
938 Mohr, C., Huffman, J. A., Cubison, M. J., Aiken, A. C., Docherty, K. S., Kimmel, J. R., Ulbrich,
939 I. M., Hannigan, M., and Jimenez, J. L.: Characterization of Primary Organic Aerosol Emissions
940 from Meat Cooking, Trash Burning, and Motor Vehicles with High-Resolution Aerosol Mass
941 Spectrometry and Comparison with Ambient and Chamber Observations, Environ Sci Technol,
942 43, 2443-2449, 10.1021/es8011518, 2009.
943
944 Mutzel, A., Poulain, L., Berndt, T., Iinuma, Y., Rodigast, M., Böge, O., Richters, S., Spindler, G.,
945 Sipilä, M., Jokinen, T., Kulmala, M., and Herrmann, H.: Highly Oxidized Multifunctional Organic
946 Compounds Observed in Tropospheric Particles: A Field and Laboratory Study, Environ Sci
947 Technol, 10.1021/acs.est.5b00885, 2015.
948
949 Ng, N. L., Canagaratna, M. R., Zhang, Q., Jimenez, J. L., Tian, J., Ulbrich, I. M., Kroll, J. H.,
950 Docherty, K. S., Chhabra, P. S., Bahreini, R., Murphy, S. M., Seinfeld, J. H., Hildebrandt, L.,
951 Donahue, N. M., DeCarlo, P. F., Lanz, V. A., Prevot, A. S. H., Dinar, E., Rudich, Y., and Worsnop,
952 D. R.: Organic aerosol components observed in Northern Hemispheric datasets from Aerosol Mass
953 Spectrometry, Atmos Chem Phys, 10, 4625-4641, DOI 10.5194/acp-10-4625-2010, 2010.
954

Ng, N. L., Brown, S. S., Archibald, A. T., Atlas, E., Cohen, R. C., Crowley, J. N., Day, D. A., Donahue, N. M., Fry, J. L., Fuchs, H., Griffin, R. J., Guzman, M. I., Herrmann, H., Hodzic, A., Iinuma, Y., Jimenez, J. L., Kiendler-Scharr, A., Lee, B. H., Luecken, D. J., Mao, J., McLaren, R., Mutzel, A., Osthoff, H. D., Ouyang, B., Picquet-Varrault, B., Platt, U., Pye, H. O. T., Rudich, Y., Schwantes, R. H., Shiraiwa, M., Stutz, J., Thornton, J. A., Tilgner, A., Williams, B. J., and Zaveri, R. A.: Nitrate radicals and biogenic volatile organic compounds: oxidation, mechanisms, and organic aerosol, Atmos. Chem. Phys., 17, 2103-2162, 10.5194/acp-17-2103-2017, 2017.

Odum, J. R., Hoffmann, T., Bowman, F., Collins, D., Flagan, R. C., and Seinfeld, J. H.: Gas/Particle Partitioning and Secondary Organic Aerosol Yields, Environ Sci Technol, 30, 2580-2585, 10.1021/es950943+, 1996.

Paatero, P., and Tapper, U.: Positive Matrix Factorization - a Nonnegative Factor Model with Optimal Utilization of Error-Estimates of Data Values, Environmetrics, 5, 111-126, DOI 10.1002/env.3170050203, 1994.

Paatero, P.: The Multilinear Engine—A Table-Driven, Least Squares Program for Solving Multilinear Problems, Including the n-Way Parallel Factor Analysis Model, Journal of Computational and Graphical Statistics, 8, 854-888, 10.1080/10618600.1999.10474853, 1999.

Palm, B. B., de Sá, S. S., Day, D. A., Campuzano-Jost, P., Hu, W., Seco, R., Sjostedt, S. J., Park, J. H., Guenther, A. B., Kim, S., Brito, J., Wurm, F., Artaxo, P., Thalman, R., Wang, J., Yee, L. D., Wernis, R., Isaacman-VanWertz, G., Goldstein, A. H., Liu, Y., Springston, S. R., Souza, R., Newburn, M. K., Alexander, M. L., Martin, S. T., and Jimenez, J. L.: Secondary organic aerosol formation from ambient air in an oxidation flow reactor in central Amazonia, Atmos. Chem. Phys. Discuss., 2017, 1-56, 10.5194/acp-2017-795, 2017.

Palm, B. B., de Sá, S. S., Day, D. A., Campuzano-Jost, P., Hu, W., Seco, R., Sjostedt, S. J., Park, J. H., Guenther, A. B., Kim, S., Brito, J., Wurm, F., Artaxo, P., Thalman, R., Wang, J., Yee, L. D., Wernis, R., Isaacman-VanWertz, G., Goldstein, A. H., Liu, Y., Springston, S. R., Souza, R., Newburn, M. K., Alexander, M. L., Martin, S. T., and Jimenez, J. L.: Secondary organic aerosol formation from ambient air in an oxidation flow reactor in central Amazonia, Atmos. Chem. Phys., 18, 467-493, 10.5194/acp-18-467-2018, 2018.

Pathak, R. K., Stanier, C. O., Donahue, N. M., and Pandis, S. N.: Ozonolysis of alpha-pinene at atmospherically relevant concentrations: Temperature dependence of aerosol mass fractions (yields), J Geophys Res-Atmos, 112, Artn D03201

Doi 10.1029/2006jd007436, 2007.

Peng, J., Hu, M., Guo, S., Du, Z., Zheng, J., Shang, D., Levy Zamora, M., Zeng, L., Shao, M., Wu, Y.-S., Zheng, J., Wang, Y., Glen, C. R., Collins, D. R., Molina, M. J., and Zhang, R.: Markedly enhanced absorption and direct radiative forcing of black carbon under polluted urban

997 environments, Proceedings of the National Academy of Sciences, 113, 4266-4271,
998 10.1073/pnas.1602310113, 2016.
999
1000 Presto, A. A., Huff Hartz, K. E., and Donahue, N. M.: Secondary Organic Aerosol Production
1001 from Terpene Ozonolysis. 2. Effect of NOx Concentration, Environ Sci Technol, 39, 7046-7054,
1002 10.1021/es050400s, 2005.
1003
1004 Pye, Pinder, R. W., Piletic, I. R., Xie, Y., Capps, S. L., Lin, Y. H., Surratt, J. D., Zhang, Z. F.,
1005 Gold, A., Luecken, D. J., Hutzell, W. T., Jaoui, M., Offenberg, J. H., Kleindienst, T. E.,
1006 Lewandowski, M., and Edney, E. O.: Epoxide Pathways Improve Model Predictions of Isoprene
1007 Markers and Reveal Key Role of Acidity in Aerosol Formation, Environ Sci Technol, 47, 11056-
1008 11064, Doi 10.1021/Es402106h, 2013.
1009
1010 Pye, H. O. T., Chan, A. W. H., Barkley, M. P., and Seinfeld, J. H.: Global modeling of organic
1011 aerosol: the importance of reactive nitrogen (NOx and NO3), Atmos Chem Phys, 10, 11261-11276,
1012 DOI 10.5194/acp-10-11261-2010, 2010.
1013
1014 Pye, H. O. T., Luecken, D. J., Xu, L., Boyd, C. M., Ng, N. L., Baker, K. R., Ayres, B. R., Bash, J.
1015 O., Baumann, K., Carter, W. P. L., Edgerton, E., Fry, J. L., Hutzell, W. T., Schwede, D. B., and
1016 Shepson, P. B.: Modeling the Current and Future Roles of Particulate Organic Nitrates in the
1017 Southeastern United States, Environ Sci Technol, 49, 14195-14203, 10.1021/acs.est.5b03738,
1018 2015.
1019
1020 Robinson, N. H., Hamilton, J. F., Allan, J. D., Langford, B., Oram, D. E., Chen, Q., Docherty, K.,
1021 Farmer, D. K., Jimenez, J. L., Ward, M. W., Hewitt, C. N., Barley, M. H., Jenkin, M. E., Rickard,
1022 A. R., Martin, S. T., McFiggans, G., and Coe, H.: Evidence for a significant proportion of
1023 Secondary Organic Aerosol from isoprene above a maritime tropical forest, Atmos Chem Phys,
1024 11, 1039-1050, DOI 10.5194/acp-11-1039-2011, 2011a.
1025
1026 Robinson, N. H., Newton, H. M., Allan, J. D., Irwin, M., Hamilton, J. F., Flynn, M., Bower, K. N.,
1027 Williams, P. I., Mills, G., Reeves, C. E., McFiggans, G., and Coe, H.: Source attribution of Bornean
1028 air masses by back trajectory analysis during the OP3 project, Atmos. Chem. Phys., 11, 9605-9630,
1029 10.5194/acp-11-9605-2011, 2011b.
1030
1031 Rollins, A. W., Browne, E. C., Min, K.-E., Pusede, S. E., Wooldridge, P. J., Gentner, D. R.,
1032 Goldstein, A. H., Liu, S., Day, D. A., Russell, L. M., and Cohen, R. C.: Evidence for NOx Control
1033 over Nighttime SOA Formation, Science, 337, 1210-1212, 10.1126/science.1221520, 2012.
1034
1035 Saha, P. K., and Grieshop, A. P.: Exploring Divergent Volatility Properties from Yield and
1036 Thermodenuder Measurements of Secondary Organic Aerosol from α-Pinene Ozonolysis, Environ
1037 Sci Technol, 10.1021/acs.est.6b00303, 2016.
1038

1039 Sarrafzadeh, M., Wildt, J., Pullinen, I., Springer, M., Kleist, E., Tillmann, R., Schmitt, S. H., Wu,
1040 C., Mentel, T. F., Zhao, D., Hastie, D. R., and Kiendler-Scharr, A.: Impact of NOx and OH on
1041 secondary organic aerosol formation from β-pinene photooxidation, Atmos. Chem. Phys., 16,
1042 11237-11248, 10.5194/acp-16-11237-2016, 2016.
1043
1044 Sen, P. K.: Estimates of the Regression Coefficient Based on Kendall's Tau, Journal of the
1045 American Statistical Association, 63, 1379-1389, 10.1080/01621459.1968.10480934, 1968.
1046
1047 Slowik, J. G., Brook, J., Chang, R. Y. W., Evans, G. J., Hayden, K., Jeong, C. H., Li, S. M., Liggio,
1048 J., Liu, P. S. K., McGuire, M., Mihele, C., Sjostedt, S., Vlasenko, A., and Abbatt, J. P. D.:
1049 Photochemical processing of organic aerosol at nearby continental sites: contrast between urban
1050 plumes and regional aerosol, Atmos Chem Phys, 11, 2991-3006, DOI 10.5194/acp-11-2991-2011,
1051 2011.
1052
1053 Spracklen, D. V., Jimenez, J. L., Carslaw, K. S., Worsnop, D. R., Evans, M. J., Mann, G. W.,
1054 Zhang, Q., Canagaratna, M. R., Allan, J., Coe, H., McFiggans, G., Rap, A., and Forster, P.: Aerosol
1055 mass spectrometer constraint on the global secondary organic aerosol budget, Atmos. Chem. Phys.,
1056 11, 12109-12136, 10.5194/acp-11-12109-2011, 2011.
1057
1058 Surratt, J. D., Chan, A. W. H., Eddingsaas, N. C., Chan, M. N., Loza, C. L., Kwan, A. J., Hersey,
1059 S. P., Flagan, R. C., Wennberg, P. O., and Seinfeld, J. H.: Reactive intermediates revealed in
1060 secondary organic aerosol formation from isoprene, P Natl Acad Sci USA, 107, 6640-6645, DOI
1061 10.1073/pnas.0911114107, 2010.
1062
1063 Tasoglou, A., and Pandis, S. N.: Formation and chemical aging of secondary organic aerosol
1064 during the β-caryophyllene oxidation, Atmos. Chem. Phys., 15, 6035-6046, 10.5194/acp-15-6035-
1065 2015, 2015.
1066
1067 Tsigaridis, K., Daskalakis, N., Kanakidou, M., Adams, P. J., Artaxo, P., Bahadur, R., Balkanski,
1068 Y., Bauer, S. E., Bellouin, N., Benedetti, A., Bergman, T., Berntsen, T. K., Beukes, J. P., Bian, H.,
1069 Carslaw, K. S., Chin, M., Curci, G., Diehl, T., Easter, R. C., Ghan, S. J., Gong, S. L., Hodzic, A.,
1070 Hoyle, C. R., Iversen, T., Jathar, S., Jimenez, J. L., Kaiser, J. W., Kirkevåg, A., Koch, D., Kokkola,
1071 H., Lee, Y. H., Lin, G., Liu, X., Luo, G., Ma, X., Mann, G. W., Mihalopoulos, N., Morcrette, J. J.,
1072 Müller, J. F., Myhre, G., Myriokefalitakis, S., Ng, N. L., O'Donnell, D., Penner, J. E., Pozzoli, L.,
1073 Pringle, K. J., Russell, L. M., Schulz, M., Sciare, J., Seland, Ø., Shindell, D. T., Sillman, S., Skeie,
1074 R. B., Spracklen, D., Stavrakou, T., Steenrod, S. D., Takemura, T., Tiitta, P., Tilmes, S., Tost, H.,
1075 van Noije, T., van Zyl, P. G., von Salzen, K., Yu, F., Wang, Z., Wang, Z., Zaveri, R. A., Zhang,
1076 H., Zhang, K., Zhang, Q., and Zhang, X.: The AeroCom evaluation and intercomparison of organic
1077 aerosol in global models, Atmos. Chem. Phys., 14, 10845-10895, 10.5194/acp-14-10845-2014,
1078 2014.
1079
1080 Tuet, W. Y., Chen, Y., Xu, L., Fok, S., Gao, D., Weber, R. J., and Ng, N. L.: Chemical oxidative
1081 potential of secondary organic aerosol (SOA) generated from the photooxidation of biogenic and

1082 anthropogenic volatile organic compounds, Atmos. Chem. Phys., 17, 839-853, 10.5194/acp-17-
1083 839-2017, 2017.
1084
1085 Ulbrich, I. M., Canagaratna, M. R., Zhang, Q., Worsnop, D. R., and Jimenez, J. L.: Interpretation
1086 of organic components from Positive Matrix Factorization of aerosol mass spectrometric data,
1087 Atmos. Chem. Phys., 9, 2891-2918, 10.5194/acp-9-2891-2009, 2009.
1088
1089 Vaden, T. D., Imre, D., Beránek, J., Shrivastava, M., and Zelenyuk, A.: Evaporation kinetics and
1090 phase of laboratory and ambient secondary organic aerosol, Proceedings of the National Academy
1091 of Sciences, 108, 2190-2195, 10.1073/pnas.1013391108, 2011.
1092
1093 Verma, V., Fang, T., Guo, H., King, L., Bates, J. T., Peltier, R. E., Edgerton, E., Russell, A. G.,
1094 and Weber, R. J.: Reactive oxygen species associated with water-soluble PM2.5 in the southeastern
1095 United States: spatiotemporal trends and source apportionment, Atmos. Chem. Phys., 14, 12915-
1096 12930, 10.5194/acp-14-12915-2014, 2014.
1097
1098 Visser, S., Slowik, J. G., Furger, M., Zotter, P., Bukowiecki, N., Canonaco, F., Flechsig, U., Appel,
1099 K., Green, D. C., Tremper, A. H., Young, D. E., Williams, P. I., Allan, J. D., Coe, H., Williams,
1100 L. R., Mohr, C., Xu, L., Ng, N. L., Nemitz, E., Barlow, J. F., Halios, C. H., Fleming, Z. L.,
1101 Baltensperger, U., and Prévôt, A. S. H.: Advanced source apportionment of size-resolved trace
1102 elements at multiple sites in London during winter, Atmos. Chem. Phys., 15, 11291-11309,
1103 10.5194/acp-15-11291-2015, 2015.
1104
1105 Weber, R. J., Sullivan, A. P., Peltier, R. E., Russell, A., Yan, B., Zheng, M., de Gouw, J., Warneke,
1106 C., Brock, C., Holloway, J. S., Atlas, E. L., and Edgerton, E.: A study of secondary organic aerosol
1107 formation in the anthropogenic-influenced southeastern United States, J Geophys Res-Atmos, 112,
1108 Artn D13302 Doi 10.1029/2007jd008408, 2007.
1109
1110 Xu, L., Guo, H., Boyd, C. M., Klein, M., Bougiatioti, A., Cerully, K. M., Hite, J. R., Isaacman-
1111 VanWertz, G., Kreisberg, N. M., Knote, C., Olson, K., Koss, A., Goldstein, A. H., Hering, S. V.,
1112 de Gouw, J., Baumann, K., Lee, S.-H., Nenes, A., Weber, R. J., and Ng, N. L.: Effects of
1113 anthropogenic emissions on aerosol formation from isoprene and monoterpenes in the southeastern
1114 United States, Proceedings of the National Academy of Sciences, 112, 37-42,
1115 10.1073/pnas.1417609112, 2015a.
1116
1117 Xu, L., Suresh, S., Guo, H., Weber, R. J., and Ng, N. L.: Aerosol characterization over the
1118 southeastern United States using high-resolution aerosol mass spectrometry: spatial and seasonal
1119 variation of aerosol composition and sources with a focus on organic nitrates, Atmos. Chem. Phys.,
1120 15, 7307-7336, 10.5194/acp-15-7307-2015, 2015b.
1121
1122 Xu, L., Middlebrook, A. M., Liao, J., de Gouw, J. A., Guo, H., Weber, R. J., Nenes, A., Lopez-
1123 Hilfiker, F. D., Lee, B. H., Thornton, J. A., Brock, C. A., Neuman, J. A., Nowak, J. B., Pollack, I.
1124 B., Welti, A., Graus, M., Warneke, C., and Ng, N. L.: Enhanced formation of isoprene-derived

organic aerosol in sulfur-rich power plant plumes during Southeast Nexus, Journal of Geophysical Research: Atmospheres, 121, 11,137-111,153, 10.1002/2016JD025156, 2016a.

Xu, L., Williams, L. R., Young, D. E., Allan, J. D., Coe, H., Massoli, P., Fortner, E., Chhabra, P., Herndon, S., Brooks, W. A., Jayne, J. T., Worsnop, D. R., Aiken, A. C., Liu, S., Gorkowski, K., Dubey, M. K., Fleming, Z. L., Visser, S., Prévôt, A. S. H., and Ng, N. L.: Wintertime aerosol chemical composition, volatility, and spatial variability in the greater London area, Atmos. Chem. Phys., 16, 1139-1160, 10.5194/acp-16-1139-2016, 2016b.

Xu, W., Han, T., Du, W., Wang, Q., Chen, C., Zhao, J., Zhang, Y., Li, J., Fu, P., Wang, Z., Worsnop, D. R., and Sun, Y.: Effects of Aqueous-Phase and Photochemical Processing on Secondary Organic Aerosol Formation and Evolution in Beijing, China, Environ Sci Technol, 10.1021/acs.est.6b04498, 2016c.

Yu, J., Cocker, D. R., Griffin, R. J., Flagan, R. C., and Seinfeld, J. H.: Gas-Phase Ozone Oxidation of Monoterpenes: Gaseous and Particulate Products, J Atmos Chem, 34, 207-258, 10.1023/a:1006254930583, 1999.

Zhang, H., Yee, L. D., Lee, B. H., Curtis, M. P., Worton, D. R., Isaacman-VanWertz, G., Offenberg, J. H., Lewandowski, M., Kleindienst, T. E., Beaver, M. R., Holder, A. L., Lonneman, W. A., Docherty, K. S., Jaoui, M., Pye, H. O. T., Hu, W., Day, D. A., Campuzano-Jost, P., Jimenez, J. L., Guo, H., Weber, R. J., de Gouw, J., Koss, A. R., Edgerton, E. S., Brune, W., Mohr, C., Lopez-Hilfiker, F. D., Lutz, A., Kreisberg, N. M., Spielman, S. R., Hering, S. V., Wilson, K. R., Thornton, J. A., and Goldstein, A. H.: Monoterpenes are the largest source of summertime organic aerosol in the southeastern United States, Proceedings of the National Academy of Sciences, 10.1073/pnas.1717513115, 2018.

Zhang, Q., Jimenez, J. L., Canagaratna, M. R., Allan, J. D., Coe, H., Ulbrich, I., Alfarra, M. R., Takami, A., Middlebrook, A. M., Sun, Y. L., Dzepina, K., Dunlea, E., Docherty, K., DeCarlo, P. F., Salcedo, D., Onasch, T., Jayne, J. T., Miyoshi, T., Shimono, A., Hatakeyama, S., Takegawa, N., Kondo, Y., Schneider, J., Drewnick, F., Borrmann, S., Weimer, S., Demerjian, K., Williams, P., Bower, K., Bahreini, R., Cottrell, L., Griffin, R. J., Rautiainen, J., Sun, J. Y., Zhang, Y. M., and Worsnop, D. R.: Ubiquity and dominance of oxygenated species in organic aerosols in anthropogenically-influenced Northern Hemisphere midlatitudes, Geophysical Research Letters, 34, Artn L13801 Doi 10.1029/2007gl029979, 2007.

Zhang, X., Cappa, C. D., Jathar, S. H., McVay, R. C., Ensberg, J. J., Kleeman, M. J., and Seinfeld, J. H.: Influence of vapor wall loss in laboratory chambers on yields of secondary organic aerosol, Proceedings of the National Academy of Sciences, 10.1073/pnas.1404727111, 2014.

Zhang, X., McVay, R. C., Huang, D. D., Dalleska, N. F., Aumont, B., Flagan, R. C., and Seinfeld, J. H.: Formation and evolution of molecular products in α-pinene secondary organic aerosol,

Proceedings of the National Academy of Sciences, 112, 14168-14173, 10.1073/pnas.1517742112, 2015.

Zheng, Y., Unger, N., Hodzic, A., Emmons, L., Knote, C., Tilmes, S., Lamarque, J. F., and Yu, P.: Limited effect of anthropogenic nitrogen oxides on secondary organic aerosol formation, Atmos. Chem. Phys., 15, 13487-13506, 10.5194/acp-15-13487-2015, 2015.

Zotter, P., El-Haddad, I., Zhang, Y., Hayes, P. L., Zhang, X., Lin, Y.-H., Wacker, L., Schnelle-Kreis, J., Abbaszade, G., Zimmermann, R., Surratt, J. D., Weber, R., Jimenez, J. L., Szidat, S., Baltensperger, U., and Prévôt, A. S. H.: Diurnal cycle of fossil and nonfossil carbon using radiocarbon analyses during CalNex, Journal of Geophysical Research: Atmospheres, 119, 2013JD021114, 10.1002/2013JD021114, 2014.

Appendix A. Data Analysis Method for Perturbation Experiments

The most challenging and important analysis is to determine if the perturbation results in a statistically significant change in the mass concentration of OA factors. We perform the following analysis to calculate the changes in the mass concentration of OA factors after perturbation, to determine if the change is significant, and to evaluate if the change is simply due to ambient variation.

The duration of one perturbation experiment is about 130min, including four periods: Amb_Bf (~30min), Chamber_Bf (~30min), Chamber_Af (~40min), and Amb_Af (~30min), as illustrated in Fig. A1. Firstly, we assume that the ambient variation is linear during both the Chamber_Bf and Chamber_Af periods (i.e., when instruments are connected to chamber and not sampling the ambient aerosol) and that the ambient variation can be represented by interpolating Amb_Bf and Amb_Af. The validity of this assumption will be discussed shortly. To obtain the slope of ambient variation, we analyze the combined Amb_Bf and Amb_Af data and use Theil-Sen estimator(Sen, 1968). The Theil-Sen estimator is a method to robustly fit a line to a set of two-dimensional points (i.e., concentration "C" and time "t" in this study). This method chooses the median of the slopes $(C_j-C_i)/(t_j-t_i)$ determined by all pairs of sample points. Compared to simple linear regression using ordinary least squares, the Theil-Sen estimator is robust and insensitive to outliers. Unless specifically noted, the slope is Appendix A is calculated from Theil-Sen estimator. Secondly, we use the slope to extrapolate the Chamber_Bf data to estimate aerosol concentration inside the chamber during the Chamber_Af period if there were no VOC injection. We refer to this estimated aerosol concentration as "extrapolated Chamber_Bf" and use it as the reference to calculate the change in aerosol mass concentration after perturbation. We extrapolate the Chamber_Bf data, instead of ambient data, because the OA concentration in chamber is lower than that in the atmosphere due to wall loss. Thirdly, we calculate the changes in the concentration of OA factors based on the difference between measured Chamber_Af data and "extrapolated Chamber_Bf".

For each perturbation experiment, after calculating the changes in the concentration of OA factors, we develop a set of criteria to determine if the changes are statistically significant and if the changes are simply due to ambient variation. The increase in the concentration of an OA factor

needs to satisfy all criteria to be considered as statistically significant and not due to ambient variation.

Criterion 1: The difference in concentration between Chamber_Af and extrapolated Chamber_Bf must be significant. We use T-test and 95% confidence interval.

Criterion 2: The slope of all data points or the first 8 data points during the Chamber_Af period is significantly different from the slope of aerosol concentration during the Chamber_Bf period. The rationale behind this criterion is that if the perturbation causes a substantial change in the concentration of an OA factor, its slope during the Chamber_Af period should be different from that during the Chamber_Bf period.

The slope of aerosol concentration during the Chamber_Af period is obtained in the following way. We calculate the slope by using (1) all data points and (2) only first 8 data points during the Chamber_Af period. This is because the concentration of factors firstly increases after perturbation and then decreases due to dilution (Fig. A1). In this case, the slope obtained by fitting all data points might be negative and will not reflect the initial increase in concentration (e.g., LO-OOA of ap_0805_1 in Fig. S9a). Using only the first few data points during the Chamber_Af period can avoid this issue. We select the first 8 data points in this period because the concentrations of total OA and OA factors typically reach the highest at the 8th point (i.e., ~16min after injection). The slope is calculated by Theil-Sen estimator.

The slope of aerosol concentration during the Chamber_Bf period is analyzed in the following way. In order to determine if the slope in Chamber_Af is significantly different from that in Chamber_Bf, we use bootstrap analysis (1000 times) to obtain a distribution of the slope of Chamber_Bf. In brief, in each random resampling of Chamber_Bf with replacement, a slope is calculated by Theil-Sen estimator. Then, 1000 times resampling provides a distribution of slope in Chamber_Bf. The 5% and 95% percentiles of the slope distribution are compared to the slope of Chamber_Af to determine if the slopes are significantly different. If the slope of Chamber_Af (from either all data points or the first 8 data points) is smaller (or larger) than the 5% (or 95%) percentile, the slopes in Chamber_Bf and Chamber_Af are significantly different.

Criterion 3: The slope of all data points or the first 8 data points during the Chamber_Af period is significantly different from the slope of ambient data (i.e., combined Amb_Bf and Amb_Af). The rationale behind this criterion is the same as the second criterion. That is, if the perturbation

causes a substantial change in the concentration of an OA factor, its slope during the Chamber_Af period should be different from that in ambient data. The procedure to obtain a distribution of slopes in the ambient data (combined Amb_Bf and Amb_Af) is same as Criterion 2.

As mentioned above, one critical assumption is that the ambient variation is linear during both the Chamber_Bf and Chamber_Af periods (i.e., when instruments are connected to chamber and not sampling the ambient aerosol) and that the ambient variation can be represented by interpolating Amb_Bf and Amb_Af. We design the following pseudo-experiment to test the validity of this assumption. In brief, we perform the same analysis as we did for the perturbation experiments, but using ambient data **only** (i.e., no perturbation data). We firstly randomly select a data point, which defines the start point of one pseudo-test. Secondly, based on the start point, we obtain the concentration of OA factors during "Amb_Bf" period, (i.e., from start point to start point + 30min), "Chamber_Bf" period (i.e., from start point + 30min to start point + 60min), "Chamber_Af" period (i.e., from start point + 60min to start point + 100min), and "Amb_Af" period (from start point + 100 min to start point + 130min). This mimics the sampling periods in a real perturbation experiment. Thirdly, we calculate the slope of ambient period (i.e., combined "Amb_Bf" and "Amb_Af" periods) and the slope of chamber period (i.e., combined "Chamber_Bf" and "Chamber_Af" periods). Fourthly, we calculate if the slope of chamber period is significantly different from the slope of ambient period. We repeat this test 1000 times and then obtain the probability of whether the slopes of chamber period and ambient period are significantly different.

Fig. A2a shows the probability that the slopes of chamber period and ambient period are not significantly different for five factors. The larger this probability is, the more reliable the linearity assumption is. The average probability is ~50% for all factors, without discernible diurnal trends. This suggest that there is ~50% chance that the linear variation assumption is valid. Since the linearity assumption is not perfect, we develop another criterion to constrain the potential influence of ambient variation on the interpretation of perturbation results.

Criterion 4: From the above pseudo-experiment on ambient data only, we can calculate the relative change in slope between "chamber period" and "ambient period" by

$$\text{relative change in slope} = \frac{\text{Slope}_{\text{Chamber}} - \text{Slope}_{\text{Amb}}}{\text{Slope}_{\text{Amb}}} \quad \text{Eqn 1}$$

In each pseudo-experiment test, we calculate a relative change in slope between "chamber period" and "ambient period". By repeating the pseudo-experiment test 1000 times, we obtain a frequency distribution of the relative change in slope for each OA factor (Fig. A2b). This frequency distribution indicates the probability that certain relative change in slope occurs due to ambient variation. Take LO-OOA as an example, the probability that the relative change in slope varies by a factor 8 due to ambient variation is ~1%. Thus, if the relative change in slope of LO-OOA in a α-pinene experiment is 8, the change is unlikely due to ambient variation. We use the 5% and 95% percentiles from the frequency distribution as the fourth criterion to determine if the changes in the concentrations of OA factors in each perturbation experiment are due to ambient variation. In other words, if the relative change in slope between Chamber_Af and ambient data in a real perturbation experiment falls outside of the 5% or 95% percentiles, the changes in the concentrations of OA factors are likely due to perturbing chamber with VOC, instead of ambient variation. This criterion strictly considers the influence of ambient variation. In general, the comparison in slope is an optimal option to account for ambient variation, because the influence of ambient variation is unlikely to coincide with the perturbation.

Based on these 4 criteria, the OA factors with significant changes in their mass concentrations as a result of perturbation are shown in Fig. 4. LO-OOA is enhanced in 14 out of 19 α-pinene experiments. However, total OA is only enhanced in 8 out of 19 α-pinene experiments. Several reasons can contribute to the different behaviors of LO-OOA and OA. Firstly, as total OA has multiple sources, the enhancement in one factor does not guarantee an enhancement of total OA. For instance, in some perturbation experiments, while LO-OOA is enhanced, the concentration of other factors steadily decreases due to ambient variation. The increase in LO-OOA and decrease in other factors compensate each other and result in a lack of enhancement in total OA. Secondly, based on the pseudo-experiment, we note that total OA is more easily affected by ambient variation than a single OA factor. For example, the 95% of the relative change in slope of total OA is 3.59, which is larger than any OA factors (Fig. A2b). Thus, the criteria for the change in total OA concentration to be considered as significant are stricter than those for a single OA factor. Thus, some experiments with significant changes in LO-OOA do not have significant changes in total OA.

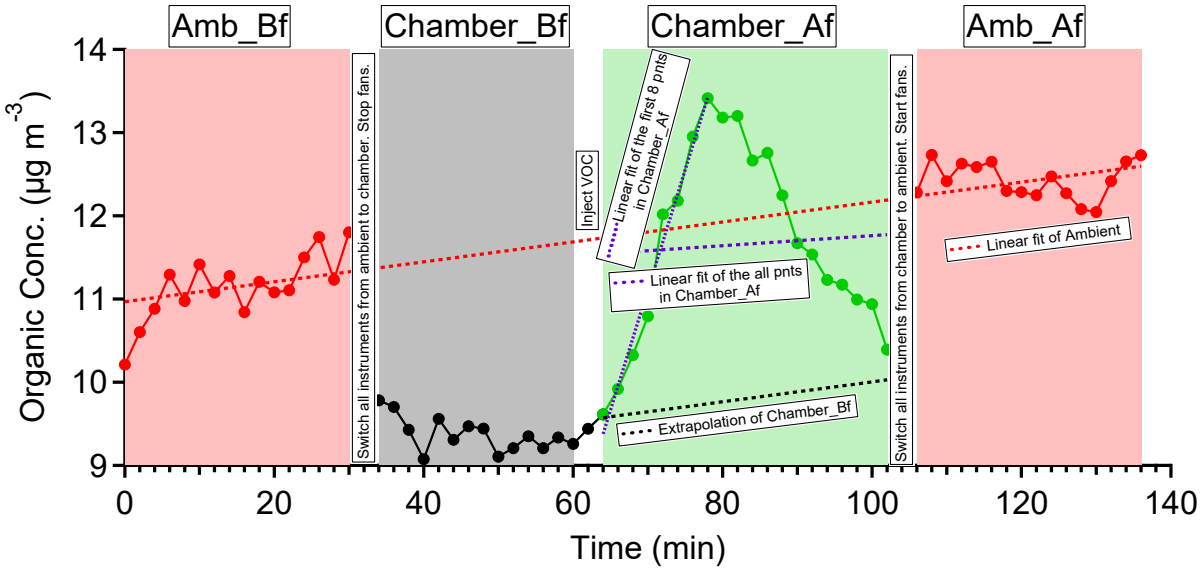

Fig. A1. Time series of OA in experiment ap_0801_1 to illustrate the analysis method. Each perturbation experiment includes four periods: Amb_Bf (~30min), Chamber_Bf (~30min), Chamber_Af (~40min), and Amb_Af (~40min). "Amb" and "Chamber" correspond to the periods when the instruments are sampling ambient and chamber, respectively. "Bf" and "Af" stand for before and after perturbation, respectively. The solid lines are measurement data. The dashed red lines are the linear fit of ambient data (i.e., combined Amb_Bf and Amb_Af). The slope is used to extrapolate Chamber_Bf data to Chamber_Af period (i.e., black dashed line). The dense dashed purple line is the linear fit of the first 8 points during the Chamber_Af period. The sparse dashed purple line is the linear fit of all data points during the Chamber_Af period. During this period, the difference between measurements (i.e., solid green data points) and extrapolated Chamber_Bf (i.e., dashed black line) represents the change in organic concentration caused by perturbation.

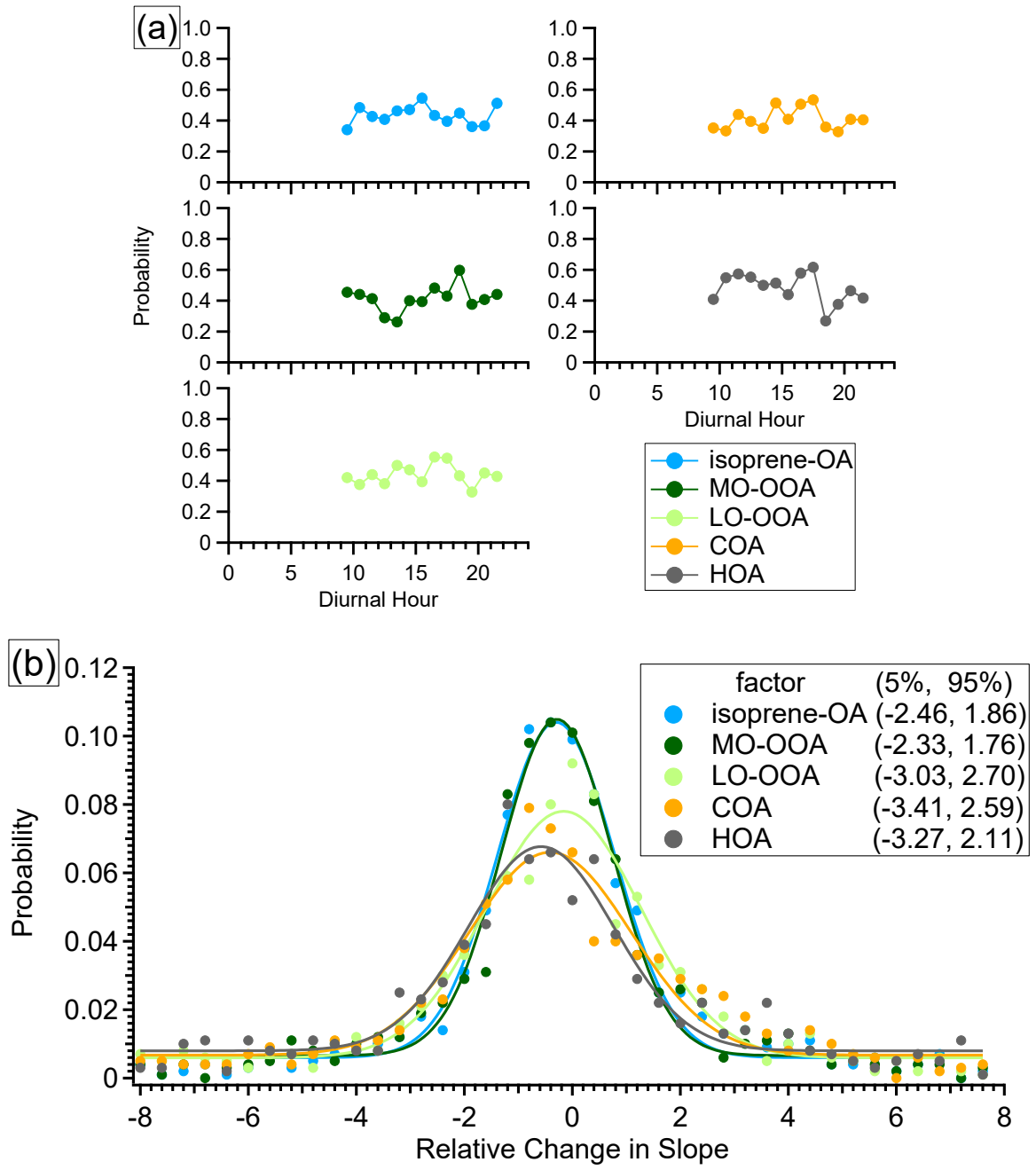

Fig. A2. (a) The diurnal trends of the probability that the slopes between ambient periods (i.e., Amb_Bf and Amb_Af periods) and chamber periods (i.e., Chamber_Bf and Chamber_Af periods) are not significantly different in the pseudo-experiment. (b) The frequency distribution of the relative change in slope. The data points are fitted using Gaussian function. The numbers in the box represent the 5% and 95% percentile of the Gaussian fit.

Appendix B. Ambient Perturbation Experiments with Acidic Sulfate Particles

Previous field observations showed strong correlation between isoprene-OA and sulfate (Xu et al., 2015a; Xu et al., 2016a; Budisulistiorini et al., 2015). Moreover, airborne measurements over power plant plumes in Georgia, U.S. observed enhanced isoprene-OA formation in the sulfate-rich power plant plume (Xu et al., 2016a). To probe the relationship between isoprene-OA and sulfate, we conducted perturbation experiments in August 2015 by injecting acidic sulfate particles (i.e., a mixture of H_2SO_4 and $MgSO_4$) into the 2 m^3 Teflon chamber. This mimics the airborne measurements over power plants, which introduce sulfate into the atmosphere (Xu et al., 2016a).

The experimental procedure in 2015 experiments is generally similar to those in 2016 experiments, but has the following modifications. Firstly, in order to avoid the depletion of species which can uptake to sulfate particles, we kept one fan on during the Chamber_Bf and Chamber_Af periods to enhance the air exchange between chamber and atmosphere. Secondly, considering the fan is on during sulfate injection to enhance mixing chamber air with ambient air, we only use the Chamber_Bf and Chamber_Af periods to calculate the changes in OA factors. The Criteria (1)(2)(4) are applied in 2015 experiments. Thirdly, the Chamber_Bf period is ~40 min in 2015 experiments, which is slightly longer than the 30 min in 2016 experiments. Fourthly, the HR-ToF-CIMS was not deployed in 2015 experiments.

The acidic sulfate seed particles were introduced into chamber by atomizing 0.88mM H_2SO_4 + 0.48mM $MgSO_4$ mixture solution from a nebulizer (U-5000AT, Cetac Technologies Inc., Omaha, Nebraska, USA). One important interference in these sulfate perturbation experiments is the trace amount of organics in solvent water [i.e., HPLC-grade ultrapure water (Baker Inc.)], which is used to prepare the H_2SO_4+$MgSO_4$ solution. These organics were injected into chamber together with sulfate. We utilize the multilinear engine solver (ME-2) to constrain the organics from solvent water (i.e., H_2O-Org). Unlike the PMF2 solver which does not require any a priori information of mass spectrum or time series, the ME-2 solver uses a priori information to reduce rotational ambiguity among possible solutions(Canonaco et al., 2013; Paatero, 1999). We obtained the reference spectrum of organic contamination (i.e., the a priori information for ME-2 solver) by atomizing the H_2SO_4+$MgSO_4$ solution directly into AMS. The ME-2 solver successfully extracted a factor (i.e., denoted as H_2O-Org factor, Fig. B1), which showed a clear enhanced concentration during atomization (Fig. B2).

A total of four experiments were performed and details are summarized in Table B1. As shown in Fig. B2, the isoprene-OA factor increases in all three daytime experiments, but not the nighttime experiment. Based on current understanding of isoprene-OA factor, this enhancement is likely due to the reactive uptake of IEPOX. The lack of enhancement in nighttime experiment is consistent with low IEPOX concentration at night (Hu et al., 2015). Our results provide direct observational evidence that acidic sulfate particles lead to increase in isoprene-OA, which supports results from previous studies (Xu et al., 2015a; Xu et al., 2016a; Budisulistiorini et al., 2015). Due to lack of measurements of gas-phase organic compounds, we are unable to identify the reactive species. Other species, such as glyoxal (Kroll et al., 2005), isoprene hydroperoxides (Liu et al., 2016), and HOMs (Ehn et al., 2014), also have the potential to uptake to acidic sulfate particles and form SOA. Future experiments with comprehensive measurements of gas-phase organic compounds can provide more insights into the identities of reactive uptake species.

We note that in non-atomizing period, the concentration of H_2O-Org factor is close to zero, but not zero. Since H_2O-Org arises from the atomizing solution, it should only exist during atomizing periods. Thus, the non-zero concentration suggests the limitation of the ME-2 solver and cautions are required when using ME-2 solver to resolve one factor based on a specific mass spectrum. This limitation does not affect the conclusion that the enhancement in isoprene-OA is likely due to the reactive uptake of organic species, as we further verify that the organic increase in three daytime perturbation experiments with sulfate particles cannot be solely explained by the organic contamination in atomizing water, from the following two aspects. For example, we atomize the solution directly into AMS and find that the Org/SO_4 ratio is 0.025. This value is significantly lower than the Org/SO_4 ratio in the three daytime sulfate perturbation experiments (i.e., 0.048-0.059), but close to the nighttime sulfate perturbation experiment (i.e., 0.022) (Fig. B4).

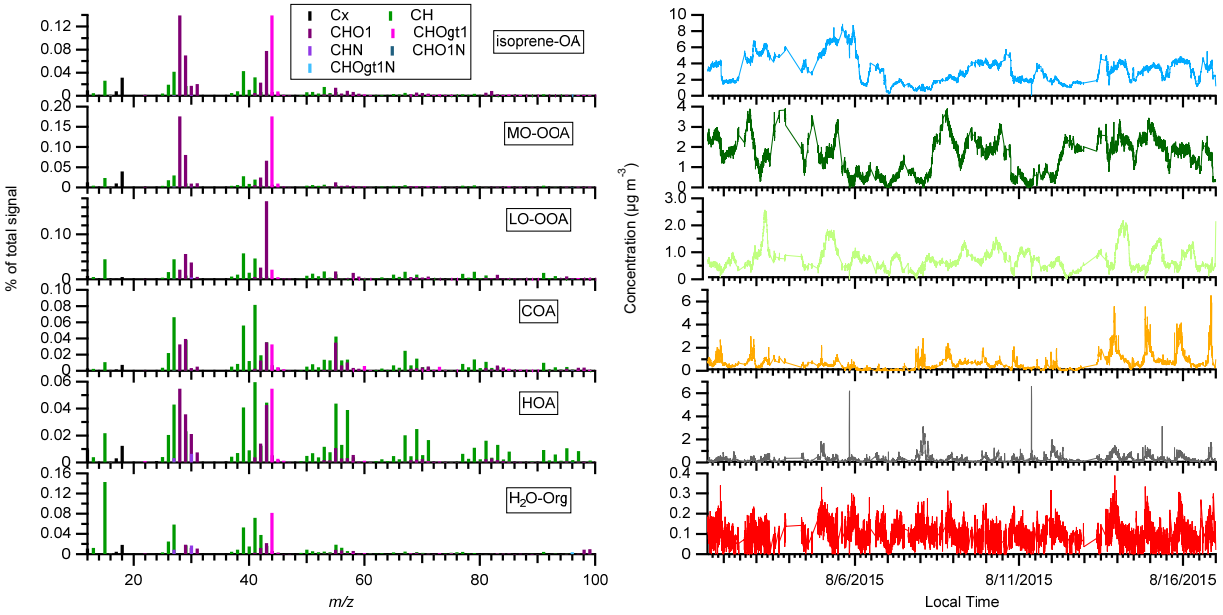

1378

1379 Fig. B1. The mass spectra and time series of OA factors in the 2015 acidic sulfate particle
1380 perturbation measurements. Note that the perturbation periods are included in the time series.

1381

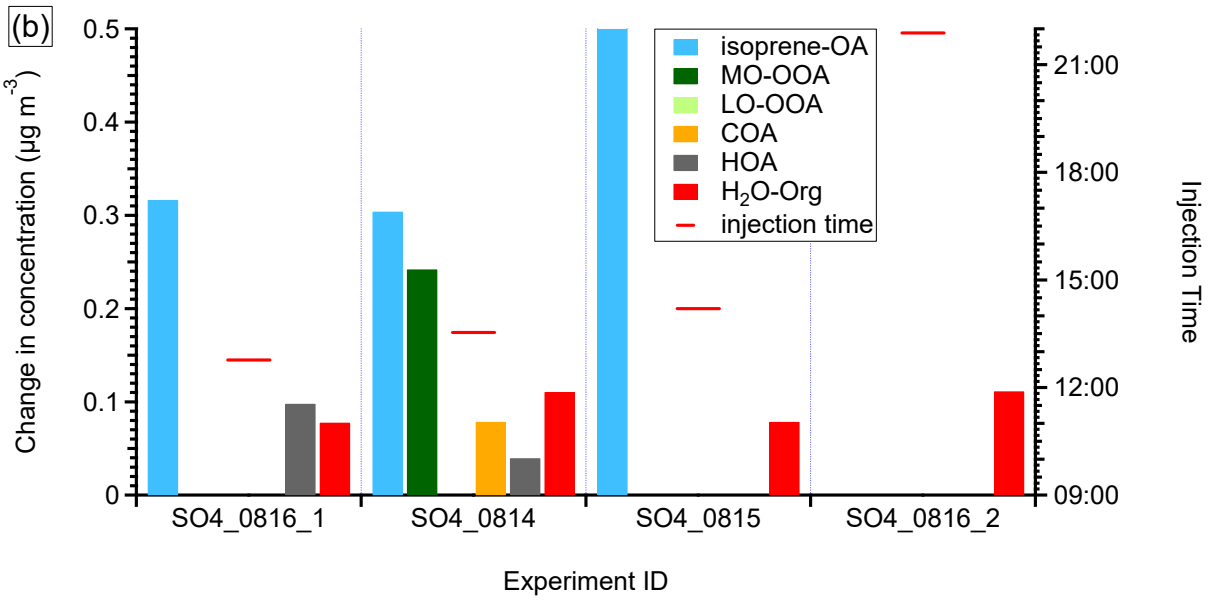

1382

1383 Fig. B2. The statistically significant changes in the concentrations of OA factors after perturbation
1384 by acidic sulfate particles. The experiments are sorted by perturbation time. The changes in
1385 concentration are the difference between measurements during the Chamber_Af period and mass
1386 concentration extrapolated from the Chamber_Bf period. A set of criteria are developed to evaluate
1387 if the changes are significant and if the changes are due to ambient variation (Appendix A). H_2O-
1388 Org factor in these sulfate perturbation experiments represents organic contaminations in
1389 atomizing water.

1390

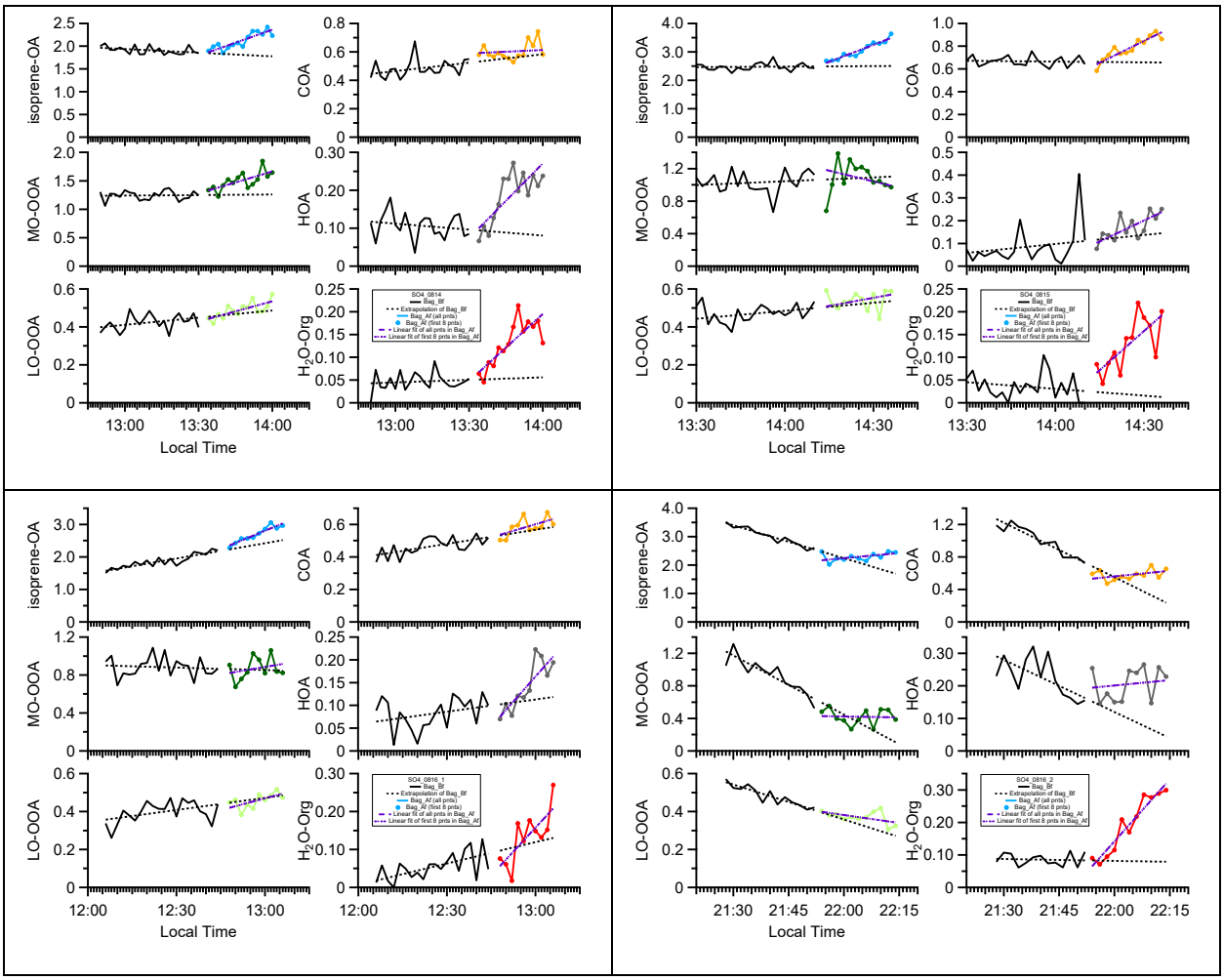

Fig. B3. Time series of OA factors in each sulfate perturbation experiment.

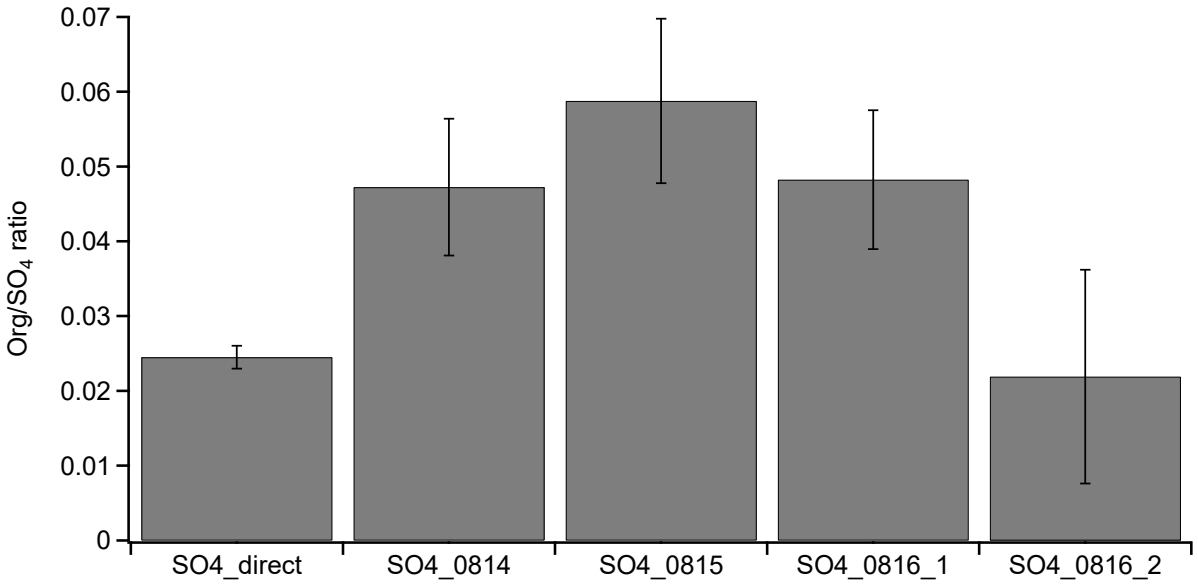

1401

1402 Fig. B4. The Org/SO_4 ratio in sulfate perturbation experiments and laboratory tests by directly
1403 atomizing H_2SO_4 + $MgSO_4$ mixture solution into AMS (i.e., SO4_direct).

1404

Table B1. Experimental conditions for sulfate perturbation experiments.

Perturbation	Expt ID[a]	Date	Injection Time	Perturbation Amount[b]	NO[c] (ppb)	NO_2[c] (ppb)	O_3[c] (ppb)
sulfate	SO4_0814	8/14/2015	13:32	16.29	0.51	5.86	59.8
	SO4_0815	8/15/2015	14:12	14.33	0.18	4.79	63.0
	SO4_0816_1	8/16/2015	12:46	14.52	0.36	4.08	53.2
	SO4_0816_2	8/16/2015	21:53	13.92	0.03	5.40	35.6

[a]Expt ID is named as "perturbation species + date + experiment number". For example, SO4_0816_1 represents the first sulfate perturbation experiment on 08/16.

[b]The unit for the perturbation in sulfate experiments is $\mu g\ m^{-3}$. The perturbation amounts of sulfate are calculated from Chamber_Af – extrapolated Chamber_bf.

[c]Average concentration during the Chamber_Af period.